PLOS ONE

RESEARCH ARTICLE

Genomic capacities for Reactive Oxygen Species metabolism across marine phytoplankton

Naaman M. Omar[1], **Katherine Fleury**[1,2], **Brian Beardsall**[1,3], **Ondřej Prášil**[4], **Douglas A. Campbell**[1]*

1 Department of Biology, Mount Allison University, Sackville, NB, Canada, **2** Faculty of Veterinary Medicine, University of Calgary, Calgary, AB, Canada, **3** Faculty of Computer Science, Dalhousie University, Halifax, NS, Canada, **4** Institute of Microbiology, Center Algatech, Laboratory of Photosynthesis, Trebon, CZ, Czech Republic

* dcampbel@mta.ca

Citation: Omar NM, Fleury K, Beardsall B, Prášil O, Campbell DA (2023) Genomic capacities for Reactive Oxygen Species metabolism across marine phytoplankton. PLoS ONE 18(4): e0284580. https://doi.org/10.1371/journal.pone.0284580

Editor: Thomas Roach, University of Innsbruck, AUSTRIA

Received: August 29, 2022

Accepted: April 4, 2023

Published: April 25, 2023

Data Availability Statement: Code, genes annotated for ROS metabolism (MergedData.csv), MetaData.csv and DataDictionary.csv are stored on https://github.com/FundyPhytoPhys/ROS_bioinfo/tree/master/ROSGenomicPatternsAcrossMarinePhytoplankton. Annotations of all genes from genomes or transcriptomes of organisms used in this study, MetaData.csv and DataDictionary.csv are stored on DRYAD (doi.org/10.5061/dryad.kh1893284) to facilitate reuse for other purposes.

Abstract

Marine phytoplankton produce and scavenge Reactive Oxygen Species, to support cellular processes, while limiting damaging reactions. Some prokaryotic picophytoplankton have, however, lost all genes encoding scavenging of hydrogen peroxide. Such losses of metabolic function can only apply to Reactive Oxygen Species which potentially traverse the cell membrane outwards, before provoking damaging intracellular reactions. We hypothesized that cell radius influences which elements of Reactive Oxygen Species metabolism are partially or fully dispensable from a cell. We therefore investigated genomes and transcriptomes from diverse marine eukaryotic phytoplankton, ranging from 0.4 to 44 μm radius, to analyze the genomic allocations encoding enzymes metabolizing Reactive Oxygen Species. Superoxide has high reactivity, short lifetimes and limited membrane permeability. Genes encoding superoxide scavenging are ubiquitous across phytoplankton, but the fractional gene allocation decreased with increasing cell radius, consistent with a nearly fixed set of core genes for scavenging superoxide pools. Hydrogen peroxide has lower reactivity, longer intracellular and extracellular lifetimes and readily crosses cell membranes. Genomic allocations to both hydrogen peroxide production and scavenging decrease with increasing cell radius. Nitric Oxide has low reactivity, long intracellular and extracellular lifetimes and readily crosses cell membranes. Neither Nitric Oxide production nor scavenging genomic allocations changed with increasing cell radius. Many taxa, however, lack the genomic capacity for nitric oxide production or scavenging. The probability of presence of capacity to produce nitric oxide decreases with increasing cell size, and is influenced by flagella and colony formation. In contrast, the probability of presence of capacity to scavenge nitric oxide increases with increasing cell size, and is again influenced by flagella and colony formation.

Introduction

Phytoplankton cells span a large size range, from picoplankton (<2μm), nanoplankton (2 to 20μm), microplankton (20 to 200μm) to macroplankton (200 to <2000μm) [1]. Cell size

Funding: NMO was supported by the Mount Allison University Rice Memorial Graduate Fellowship (2020) and a New Brunswick Innovation Foundation STEM Graduate Award (2020). KF was supported by NSERC Indigenous Undergraduate Summer Research Award (2019) and the MITACS GlobalLink internship (2019). BB was supported by the Canada Research Chair in Phytoplankton Ecophysiology fund. DAC was supported by the Canada Research Chair in Phytoplankton Ecophysiology (11-1-115630-63120) and by the Microbiology Institute of the Czech Academy of Science through project CZ.02.2.69/0.0/0.0/16_027/0007990 of the European Union Researcher Mobility program. The funders had no role in study design, data collection and analysis, decision to publish, or preparation of the manuscript.

Competing interests: The authors have declared that no competing interests exist.

interacts with multiple selective pressures, including cellular metabolic rate, light absorption, nutrient uptake, cell nutrient quotas, trophic interactions and diffusional exchanges with the environment [1–5]. Beyond simple size, cell shapes and growth forms influence diffusional exchanges between cells and their environment [6].

Characteristics of reactive oxygen species

Phytoplankton both produce and scavenge Reactive Oxygen Species (ROS), both within and outside the cell membrane, enzymatically and non-enzymatically. Some ROS readily cross the cell membrane, connecting intra- and extra-cellular pools. Other ROS rarely cross cell membranes and therefore intra- and extra-cellular pools are at least partially segregated (Table 1).

Superoxide ($O_2^{\bullet-}$), a radical anion generated through the monovalent reduction of O_2 to $O_2^{\bullet-}$ [29], is highly reactive [30] with organic compounds including thiols [31], and with metals [32, 33]. As the first ROS in a sequential series of reductions of O_2, $O_2^{\bullet-}$ is a 'gateway' to production of other ROS. $O_2^{\bullet-}$ is produced both inside and outside a cell [34–39], but shows limited diffusion across the hydrophobic cell membrane [17]. Multiple oxidases (S2 Table) reduce O_2 and generate either H_2O [40], or alternately $O_2^{\bullet-}$ and/or Hydrogen Peroxide (H_2O_2) [41, 42]. Biogenic production of extracellular ROS is significant in marine environments [7, 43–51], and $O_2^{\bullet-}$ in coastal waters is primarily attributable to extracellular production mediated by eukaryotic phytoplankton [52]. Some extracellular $O_2^{\bullet-}$ production likely contributes to cell growth [53].

Two known enzymes mediate conversion of $O_2^{\bullet-}$ to H_2O_2; the ubiquitous dismutation of $O_2^{\bullet-}$ catalyzed by diverse Superoxide Dismutases (SOD) or the less prevalent reduction of $O_2^{\bullet-}$, catalyzed by Superoxide Reductase (SOR) at the expense of metabolic reductant. $O_2^{\bullet-}$ also dismutates spontaneously to produce H_2O_2 and O_2 [54], although [55] found that ~52% of dark $O_2^{\bullet-}$ production likely undergoes oxidation back to O_2. Extracellular production of $O_2^{\bullet-}$ thus contributes to extracellular H_2O_2 pools [47, 48, 56, 57].

H_2O_2 passively traverses cell membranes [58], primarily through aquaporins [10–13], allowing exchange of intracellular and extracellular pools of H_2O_2, although cells can maintain a concentration gradient between internal and external H_2O_2 [59]. H_2O_2 is acutely toxic to most cells in the range of 10^{-5} to 10^{-4} mol L^{-1} [58], reacting with thiols and methionine [31] and interfering with gene expression [60]. Cytotoxic effects of H_2O_2, including lipid damage, are however, primarily caused by H_2O_2 dismutating into the Hydroxyl Radical ($HO^{\bullet}$), which is strongly oxidative [9].

Multiple oxidases are important in producing H_2O_2 (S2 Table), but abiotic processes, including rainfall, may be dominant sources of extracellular H_2O_2 in seawater [61–63]. H_2O_2 concentrations in seawater follow a diurnal cycle with a peak at mid-day [61, 64, 65], suggesting significant direct or indirect photochemical or photobiological generation of H_2O_2. Heterotrophs do not contribute much H_2O_2 production but mediate H_2O_2 decomposition [66]. H_2O_2 also decomposes spontaneously, though slowly, into water and oxygen [67], and contributes significantly to the redox cycling of copper and iron in seawater [68, 69].

Despite its radical nature and ability to react with biomolecules, $^{\bullet}NO$ functions widely as a signaling molecule [70–72]. $^{\bullet}NO$ is produced both biogenically through arginine dependent Nitric Oxide Synthases (NOS) or Nitric Oxide Associated Proteins (NOA) [73], as well as through abiotic processes including nitrite photolysis [74]. $^{\bullet}NO$ can be enzymatically scavenged through Nitric Oxide Dioxygenase (NOD) or Nitric Oxide Reductases (NOR) [75] (S2 Table), and may also react non-enzymatically with reduced glutathione (GSH) to form S-nitrosoglutathione (GSNO) [21, 76]. Most cellular damage mediated by $^{\bullet}NO$ is attributed to the

Table 1. Diffusion and stability of different ROS.

ROS	ROS Symbol	Concentration in Seawater (M)	Concentration Citation	Diffusion Distance (nm)	Diffusion Distance Citation	Lifetime (s)	Lifetime Citation	Crosses Cell Membrane	Crosses Cell Membrane Citation	Abiotic Production (Ms^{-1})	Abiotic Production Rates Citation	Diffusion Coefficient (um^2us)	Diffusion Coefficient Citation
Hydrogen Peroxide	H_2O_2	10^{-9} to 10^{-6}	[7, 8]	NA	NA	hours to days	[7–9]	Yes	[10–13]	1e-13	[14]	1500	[15]
Superoxide	$O_2^{\bullet-}$	10^{-12} to 10^{-9}	[7, 16]	320	[9]	ms to minutes	[7, 16]	No	[17]	1e-14	[14]	210	[18]
Nitric Oxide	$NO^{\bullet}$	10^{-12} to 10^{-10}	[16, 19]	NA	NA	seconds	[16, 20]	Yes	[21]	1e-13	[16]	2210	[22]
Hydroxyl Radical	$HO^{\bullet}$	10^{-18} to 10^{-15}	[7]	4.5	[9]	μs	[7]	No	[23]	3e-22	[24]	NA	NA
Singlet Oxygen	$^1O_2$	10^{-14} to 10^{-13}	[25]	82	[9]	μs	[9]	NA	NA	NA	NA	2100	[26]
Peroxynitrite	$ONOO^-$	10^{-12} to 10^{-11}	[16]	NA	NA	ms	[16, 27]	Yes	[28]	1e-11	[16]	NA	NA

https://doi.org/10.1371/journal.pone.0284580.t001

reaction of $^{\bullet}NO$ with $O_2^{\bullet-}$ to produce Peroxinitrite ($ONOO^-$) but this reaction is limited by the low extracellular concentration of $^{\bullet}NO$ in seawater [16].

Other important ROS, Singlet Oxygen ($^1O_2$), Peroxynitrite ($ONOO^-$) and $HO^{\bullet}$ are not known to be directly produced nor scavenged by enzymatic processes [58, 77–81]. Because of the high reactivity of $HO^{\bullet}$, it is unlikely that there are any scavengers dedicated to $HO^{\bullet}$ specifically [58], although reactions with dissolved organic matter non-specifically scavenge extracellular $HO^{\bullet}$ [82].

The black queen hypothesis

The Black Queen Hypothesis states that loss of function mutations may proceed so long as some interacting community members retain the function, and the function can occur outside a given cell [83]. The Black Queen Hypothesis was formulated on the basis of *Prochlorococcus*, which lost the genes encoding enzymes which scavenge H_2O_2. Instead, *Prochlorococcus* allows H_2O_2 outwards across the cell membrane to be dealt with by community members retaining the capacity to scavenge H_2O_2, thus saving *Prochlorococcus* the cost of maintaining the genes and metabolism for scavenging H_2O_2 [83, 84]. Growth and survival of *Prochlorococcus* indeed improves when co-cultured with 'helper' bacteria which carry genes for catalase [84–87].

Hypotheses and significance

Given that ROS show differential abilities to cross cell membranes, and have widely different diffusion distances before destruction [88], we sought to study whether cell radius, colony formation, flagella, or diatom cell shape influence genomic allocations to ROS production and scavenging across diverse marine phytoplankters.

Hypothesis 1 **Cell radius across phytoplankton taxa does not influence the fraction of total gene content encoding $O_2^{\bullet-}$ production, nor scavenging.** $O_2^{\bullet-}$ is highly toxic and does not readily cross biological membranes [17], so diffusional losses of $O_2^{\bullet-}$ from cells are limited, and cells need to retain capacity for detoxification of $O_2^{\bullet-}$ across cell sizes.

Hypothesis 2 **Large phytoplankton allocate a smaller fraction of their total gene content to H_2O_2 and $^{\bullet}NO$ production and a larger fraction of their total gene content to H_2O_2 and $^{\bullet}NO$ scavenging.** H_2O_2 and $^{\bullet}NO$ have relatively low reactivity, with long intracellular and extracellular lifetimes leading to long potential diffusion paths before destruction. Both H_2O_2 and $^{\bullet}NO$ are uncharged and readily cross cell membranes (Table 1). Large cells have longer intracellular diffusional paths and a lower surface to volume ratios than do smaller cells [1]. Large cells are thus less prone to diffusional losses of intracellular H_2O_2 and $^{\bullet}NO$. To maintain H_2O_2 and $^{\bullet}NO$ homeostasis in the face of slower diffusional losses of H_2O_2 or $^{\bullet}NO$ out of the cells to the environment, large phytoplankton may have a smaller fraction of their gene contents encoding H_2O_2 and $^{\bullet}NO$ production. In contrast, loss of function mutations on enzymes that scavenge H_2O_2 and $^{\bullet}NO$ would be more deleterious in large cells than in smaller cells [83, 84].

Hypothesis 3 **Flagellated phytoplankton have a larger fraction of their total gene content encoding H_2O_2 and $^{\bullet}NO$ production, and a smaller fraction of their total gene content encoding H_2O_2 and $^{\bullet}NO$ scavenging.** Increased motility in flagellated cells allows movement away from cytotoxic levels of H_2O_2 and $^{\bullet}NO$, possibly complementing scavenging.

Hypothesis 4 **Colony forming phytoplankton have a smaller fraction of their total gene content encoding H_2O_2 and $^{\bullet}NO$ production, and a larger fraction of their total gene content encoding H_2O_2 and $^{\bullet}NO$ scavenging.** Cell spacing in colony forming phytoplankton is so small that the diffusional spheres of H_2O_2 or $^{\bullet}NO$ diffusing outwards from cells overlap with

nearby cells [88], thereby shifting the requirements to maintain homeostasis within cells of a colony.

Hypothesis 5 **Pennate Diatoms allocate a larger fraction of their total gene content to H_2O_2 and $^{\bullet}NO$ production, and a smaller fraction of their total gene content to H_2O_2 and $^{\bullet}NO$ scavenging than do Centric Diatoms.** Pennate diatoms have a small minimum radii even at large biovolumes due to their elongated shape [89]. This cell shape of pennate diatoms allows for more diffusion of H_2O_2 and $^{\bullet}NO$ across the cell membrane due to the shorter mean diffusion paths to the cell surface and high surface area to volume ratio. To maintain homeostasis, pennate diatoms may have a larger fraction of their total gene content for H_2O_2 and $^{\bullet}NO$ production compared to centric diatoms. In contrast, pennate diatoms may have a smaller fraction of their gene content for H_2O_2 and $^{\bullet}NO$ scavenging, compared to centric diatoms.

Our work analyzed the fraction of the total genes in a genome or transcriptome associated with the metabolism of a particular ROS. The presence or absence of genes encoding specific ROS metabolizing enzymes may be caused by genetic drift, or may relate to a selective advantage linked to other metabolites of the same enzyme, rather than an enzymatic role in ROS metabolism, *per se*. Furthermore, the presence of a gene in a genome does not necessarily mean the encoded enzyme will be active, and closely related enzymes may mediate different activities in different organisms. The influence of non-enzymatic pathways such as carotenoids or tocopherols [42, 90, 91] likely affect the hypotheses listed above, but were beyond the frame of this study.

Methods

Data dictionary

S1 Table contains a data dictionary of variable names used in our analysis, their definitions and locations in code and data objects.

Bioinformatic pipeline

We downloaded Genomes and/or Transcriptomes of 146 diverse marine phytoplankton (S3 Table) from the National Center for Biotechnology Information (NCBI) [92]; Joint Genome Institute (JGI) [93, 94]; iMicrobe [95], European Nucleotide Archive (ENA) [96]; pico-PLAZA [97], 1000 Plants (1KP) [98]; and the Reef Genomics Database [99] (Fig 1).

We implemented an automated pipeline using Snakemake [100] to pass gene sequences from downloaded genomes or transciptomes, in.fasta format, to eggNOG-Mapper 2.0.6 [101, 102] and then used the DIAMOND algorithm [103] and the eggNOG 5.0 database [104], to annotate potential orthologs in each analyzed genome or transcriptome, using the following parameters: seed_ortholog_evalue = 0.001, seed_ortholog_score = 60, tax_scope = "auto," go_evidence = "non-electronic," query_cover = 20 and subject_cover = 0. The annotation generated for each gene model included (when available): the name of the matching ortholog (coded by eggNOG as 'seed_eggNOG_ortholog'); E-value (coded by eggNOG as 'seed_ortholog_evalue'); Score (coded by eggNOG as 'seed_ortholog_score'); EC number (coded by eggNOG as 'EC'); Kegg Orthology (KO) number (coded by eggNOG as 'KEGG_ko'); Kegg Pathway (coded by eggNOG as 'KEGG_Pathway'); Kegg Module (coded by eggNOG as 'KEGG_Module'); Kegg Reaction (coded by eggNOG as 'KEGG_Reaction'); Kegg Reaction Class (coded by eggNOG as 'KEGG_rclass'); the predicted protein family (coded by eggNOG as 'PFAMs'); Gene Ontology (GO) annotation (coded by eggNOG as 'Gos'); as well as a description from eggNOG of the source organism of the matching ortholog (coded by eggNOG as 'best_og_desc'). Note that comparison of sequences to the eggNOG 5.0 database

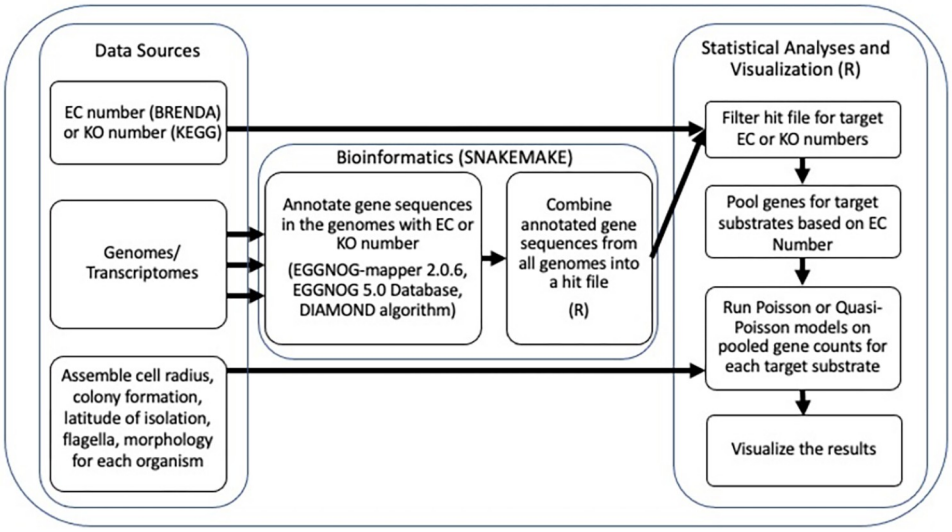

Fig 1. Summary flowchart of methods.

https://doi.org/10.1371/journal.pone.0284580.g001

generates non-supervised orthology annotations, and is subject to error if the underlying eggNOG annotation was inaccurate, or for functionally divergent orthologous gene sequences. The output of automatically annotated orthologs, from each genome or transcriptome, from the bioinformatic pipeline was compiled into one file CombinedHits.csv (to be submitted to the DRYAD database to support alternate analyses) (Fig 1).

Overview of analysis of annotated genes

CombinedHits.csv was imported into a data frame (coded as 'CombinedHits') for analysis using R [105] running under RStudio [106], using the 'tidyverse' [107], 'broom' [108], 'magrittr' [109], 'dplyr' [110], 'rcompanion' [111], 'gmodels' [112], 'stats' [105], 'AER' [113] and 'smatr' [114] packages, and the 'logit2prob' function [115]. Graphics and tables were generated using the 'ggplot2' [116], 'cowplot' [117], 'glue' [118], 'kableExtra' [119], 'corrplot' [120], 'ggfortify' [121, 122], and 'ggforce' [123] packages (Fig 1). Formatted outputs were generated from Rmarkdown files using the 'knitr' [124–126] and 'bookdown' [127] packages.

In parallel we assembled metadata from the literature and culture collection databases for each phytoplankter for which we obtained a genome or transcriptome; including the cell radii in μm from 100% of organisms (S1 Fig); colony formation for 84% of organisms; cell shape from diatoms from 100% of diatoms; presence or absence of flagella as an index of potential motility from 100% of organisms; the genome size from all genomes; the total number of predicted gene models from 97% of organisms; and the total number of nuclear genes encoding ribosomal components from 100% of organisms (S3 Table); all stored in CellGenomeMetrics.csv (submitted to the DRYAD database to support alternate analyses; doi.org/10.5061/dryad.kh1893284) (Fig 1). For organisms for which only transcriptomes were available, we only included datasets for which the total number of detected different transcripts was available, as a proxy for the total number of predicted genes. Strains of brackish origin were included but we did not include obligate freshwater strains in our analyses.

Citations were managed using the Zotero (www.zotero.org) open access reference manager connected to Rstudio using the 'citr' [128] package. The Zotero library of citations for this paper is available at (https://www.zotero.org/groups/2333131/ros_phytoplankton).

We compared the Enzyme Commission Number (EC number) from CombinedHits to the BRENDA enzyme database [129] to identify enzymes annotated by BRENDA as 'natural product' or 'natural substrate' for H_2O_2, $O_2^{\bullet-}$ or $^{\bullet}NO$ *in vivo* (S2 Table; Fig 1). We then used the EC Number to filter 'CombinedHits' to generate a subset containing only those orthologs encoding enzymes directly mediating metabolism, Production or Scavenging, of H_2O_2, $O_2^{\bullet-}$ and $^{\bullet}NO$.

From the 'CombinedHits' data frame, we filtered out some enzymes where the BRENDA annotations of 'natural product' or 'natural substrate' was questionable, in particular:

- Superoxide oxidase (EC:1.10.3.17) carries a BRENDA annotation of 'natural product' for $O_2^{\bullet-}$, despite the BRENDA citation stating that $O_2^{\bullet-}$ production from superoxide oxidase was only documented *in vitro* with an excess of ubiquinone [130].
- D-amino-acid oxidase was removed from counts of genes encoding H_2O_2 production, as the enzyme does not produce H_2O_2 *in vivo* [131].
- Bacterial non heme ferritin is listed under H_2O_2 production and scavenging as it produces H_2O_2 in the first of a two-step reaction and scavenges H_2O_2 in the second step [132].

From the subset of 'CombinedHits' of enzymes annotated for ROS metabolism, we grouped orthologs together by EC number and their Kegg Orthology number (KO number) and determined the occurrences of individual orthologs encoding each EC number, or KO number when EC number was not available, in a given organism. We merged this data subset with CellGenomeMetrics.csv to generate a dataset of genes encoding ROS metabolizing enzymes, as defined by the EC or KO number, along with characteristics of the source organism, combined into 'MergedData.' From the 'CombinedHits' data frame, we extracted and counted all genes annotated by eggNOG as ribosomal (Genes with the GO annotation 'GO:0005840'; coded as Ribosome_count), which we subsequently use as a proxy for housekeeping genes.

H_2O_2, $O_2^{\bullet-}$ and $^{\bullet}NO$ differ in reactivity, stability, diffusion distance, effects on biomolecules and roles in cell signaling (Table 1). We therefore generated the total gene counts coding for the production or scavenging of each different ROS in a given organism, which were used to generate Poisson or Quasi-Poisson regressions (Fig 1). For $^{\bullet}NO$, we also ran Binomial probability models to infer the cell size at which organism has an equal probability of having (or not having) the genomic capacity to encode nitric oxide production or scavenging. These presence/absence analyses were not run for H_2O_2 and $O_2^{\bullet-}$ as all eukaryotic organisms either ubiquitously had the genomic capacity to scavenge H_2O_2 and $O_2^{\bullet-}$; and to produce H_2O_2; whereas no organism had specific genomic capacity to produce $O_2^{\bullet-}$.

Data validation & justification of statistical analyses

Data from both genomes and transcriptomes were used in this analysis to gain wider representation from more taxa (S1 Fig). Data from the taxa with the largest radii were derived wholly from transcriptomes. Aside from the prokaryote genomes, sourced solely from within the 45˚ north south latitude band, the sampled phytoplankton did not exhibit taxonomic biases in source latitude of isolation, but were primarily coastal (S2 Fig). For 40 organisms we had both genomic and transcriptomic data, which we used to test assumptions on data distributions (S3 Fig). As expected, data coverage from paired genomes and transcriptomes derived from the same organism correlated well. Therefore, both genomic and transcriptomic data were available from the same organism, we used genomic data in subsequent analyses (S3 Table), but we used data from transcriptomes when genomes were not available. We validated the gene annotations generated by the snakemake bioinformatic pipeline by comparing the total number of genes encoding ROS metabolism data from a subset of 'CombinedHits.csv' to the total number

of genes encoding ROS metabolism data from a manually annotated dataset generated during a pilot project (S3 Fig) [133, 134].

As expected, S4 Fig shows a strong correlation (Correlation of 0.87, $p = 1.6\times10^{-49}$) between manually generated 'ROSGene_count' and the automated 'ROSGene_count' from the snakemake pipeline.

S5 Fig shows that the frequencies of counts of genes encoding the metabolism of $O_2^{\bullet-}$, H_2O_2 or $^{\bullet}NO$ within an organism are not normally distributed (Shapiro-Wilk Test [135] with a p-value of 6.4×10^{-30} for $O_2^{\bullet-}$ scavenging, 9.4×10^{-24} for H_2O_2 production, 5×10^{-25} for H_2O_2 scavenging, 1.2×10^{-18} for $^{\bullet}NO$ production and 1.5×10^{-30} for $^{\bullet}NO$ scavenging). The frequencies of gene counts instead follow Poisson distributions. Therefore, for subsequent analyses we used Poisson or Quasi-Poisson regressions to compare the counts of genes that encode the production or scavenging of $O_2^{\bullet-}$, H_2O_2 or $^{\bullet}NO$ within an organism to $\log_{10}$ of the median cell radius in μm. Code used to produce the Poisson and Quasi-Poisson models is on https://github.com/FundyPhytoPhys/ROS_bioinfo/tree/master/ROSGenomicPatternsAcrossMarinePhytoplankton.

Quasi-Poisson regressions were used when the Poisson regression was over-dispersed (dispersion > 1, $p < 0.05$) as determined by the 'AER' package [113]. A Poisson regression followed by a chi-squared test, or a Quasi-Poisson regression followed by an F-test, was used to obtain p-values [136], with an alpha value of ≤ 0.05 as the threshold for statistical significance of regressions; and a pseudo-R^2 was calculated using the McFadden R^2 method [137].

The total number of genes in each organism increased with the median cell radius, and also varied among the taxonomic lineages (coded as 'Phylum') (Fig 2). Taxonomic lineage, in turn, interacts strongly with the median cell radius. For our analyses, we sought to detect effects of cell radius upon the fraction of total genes encoding ROS metabolism. We therefore included an offset of the total number of genes in the organism in the Poisson or Quasi-Poisson regressions, which is equivalent to normalizing the number of genes encoding the production or scavenging of H_2O_2, $O_2^{\bullet-}$ or $^{\bullet}NO$, to the total number of genes in the organism ('GeneModel_count'). We thereby offset the general increase in 'GeneModel_count' with increasing the median cell radius. Because of the strong interaction between the median cell radius and taxonomic lineage (S1 Fig), we did not include Phylum as a co-variate in our subsequent regressions of normalized gene counts vs. median cell radius. Thus, we did not analyze specific influences of Phylum upon gene counts for ROS metabolism. Poisson or Quasi-Poisson regressions were run both with or without 'Colony' and 'Flagella' as co-variates.

The total number of ribosomal genes did not increase with median cell radius, but did vary with taxa (S6 Fig). Therefore, we also normalized the number of genes encoding the production or scavenging of H_2O_2, $O_2^{\bullet-}$ or $^{\bullet}NO$, to the total number of ribosomal genes in the organism ('Ribosome_count'), as a proxy for housekeeping genes. Because median cell radius and taxonomic lineage did not interact in this plot, we included Phylum, or 'Colony' and 'Flagella,' as co-variates in our Poisson or Quasi-Poisson regressions of normalized ribosomal gene counts vs. median cell radius.

To further investigate possible influences of colony formation, the presence of flagella or diatom cell shape (pennate or centric), independent of cell size, upon the fraction of genes that encode the metabolism of H_2O_2, $O_2^{\bullet-}$ or $^{\bullet}NO$, we used a Wilcoxon test [138] after binning data across all diatom sizes.

Results and discussion

Superoxide

Although there are enzymes that specifically produce $O_2^{\bullet-}$ [139], in the marine phytoplankton genomes and transcriptomes that we analyzed, we did not detect any genes that encode for

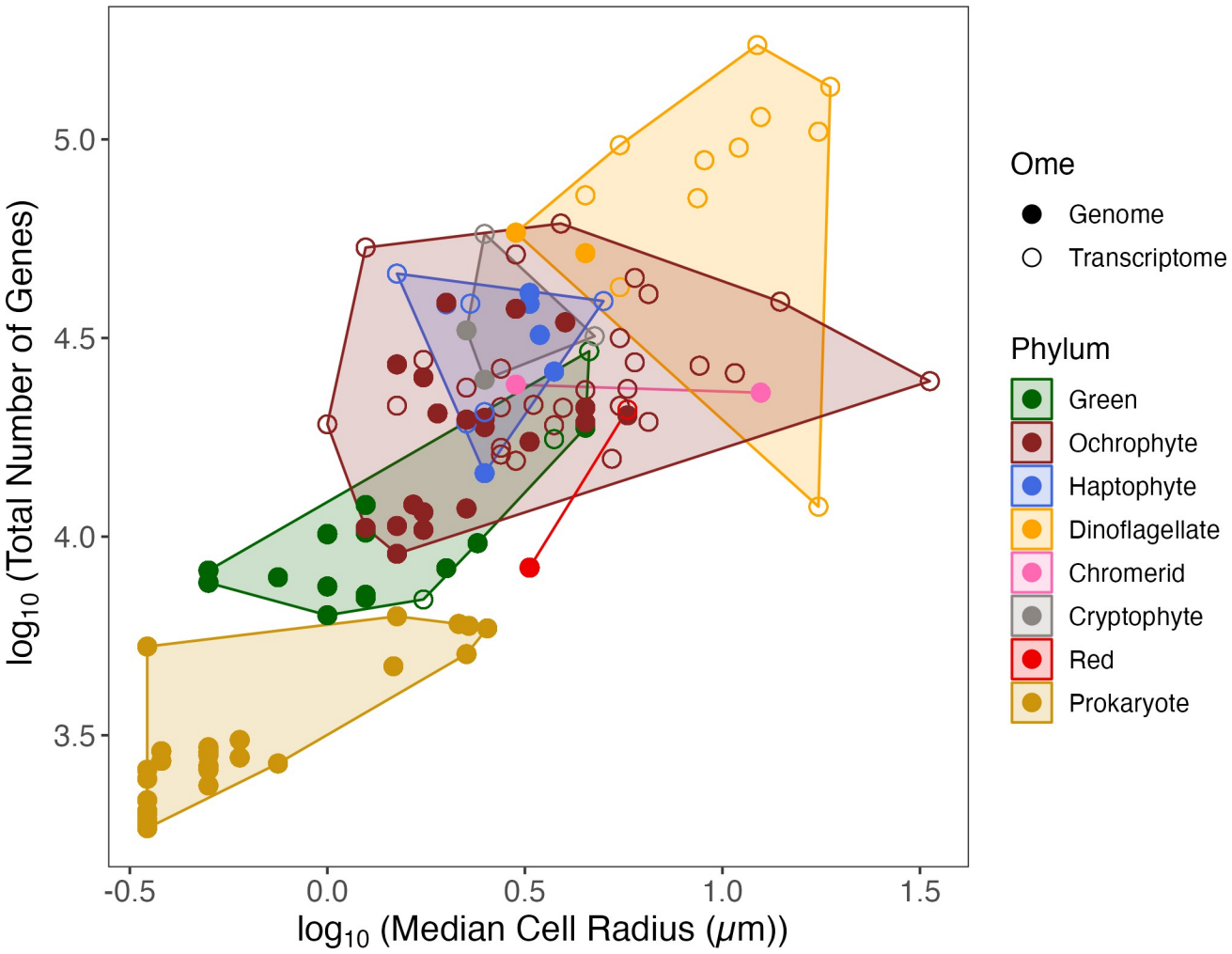

Fig 2. Comparison of log_{10} of the total number of genes in an organism ('log_GeneModels_count') to log_{10} of the median cell radius in μm ('log_Radius_um'). Colour corresponds to the taxonomic lineage ('Phylum'), whereas symbol shape corresponds to the source of the data, whether Genome or Transcriptome ('Ome'). Citations for data sources are in S3 Table.

https://doi.org/10.1371/journal.pone.0284580.g002

such enzymes (S2 Table), based on the BRENDA annotation. It is however worth noting the presence of genes annotated as encoding NADPH Oxidase (NOX) in some phytoplankton genomes. NOX can produce either H_2O_2 or $O_2^{\bullet-}$ depending on the NOX isoform. NOX is included in our analyses as a H_2O_2 producer, in accordance with the BRENDA annotation of the enzyme (S2 Table). Further analyses of the detected NOX isoforms might identify whether they include isoforms that produce $O_2^{\bullet-}$. Sequences that are similar to Glutathione Reductase (GR) have been documented to produce enzymes that produce extracellular $O_2^{\bullet-}$ in the diatom *Thalassiosira oceanica* [139]. We found sequences annotated as GR across all phytoplankton genomes (S4 Table), which likely include genes encoding enzymes producing $O_2^{\bullet-}$. Phytoplankton may need to maintain working extracellular concentrations of $O_2^{\bullet-}$, since decreasing the extracellular concentration of $O_2^{\bullet-}$ can hinder cell growth [48]. [48] further explains that the downregulation of Superoxide Dismutase (SOD, EC:1.15.1.1) genes at peak light levels by *Prochlorococcus* [140] may allow *Prochlorococcus* to maintain 'working levels' of extracellular $O_2^{\bullet-}$. Beyond putative enzymatically mediated production of $O_2^{\bullet-}$, non-enzymatic processes

associated with cells can also produce $O_2^{\bullet-}$ to variable extents, notably from side-reactions of electron transport [38, 141, 142] particularly under stress conditions.

Given that the $O_2^{\bullet-}$ is poorly diffusible across membranes, intracellularly produced $O_2^{\bullet-}$ has to be scavenged to limit detrimental reactions of $O_2^{\bullet-}$ [143]. As a result, the analyzed phytoplankton universally maintain genomic capacity encoding the ubiquitous $O_2^{\bullet-}$ scavenging enzyme SOD (S8 Fig), with the exception of a single transcriptome from *Micromonas polaris*. Genes annotated as encoding the enzyme Superoxide Oxidase (SOO, EC:1.10.3.17) were present in a few diatom species (*Leptocylindrus danicus*, *Chaetoceros curvicetus* and *Thalassiosira minuscula* CCMP1093) and prokaryotes (*Crocosphaera* spp.). Genes encoding the enzyme Superoxide Reductase (SOR, EC:1.15.1.2) were detected in some diatoms (*Pseudo-nitzschia fradulenta* WWA7 and *Seminavis robusta* D6), and in the haptophyte *Pleurochrysis carterae* CCMP456. BLAST searches support these annotations of genes for SOO and SOR in the genomes of some phytoplankters. These results should be confirmed by enzyme assays, to identify if the genes indeed encode active enzymes. Finer trends in genomic allocations to $O_2^{\bullet-}$ scavenging may emerge among the metallo-forms of SOD [144]. For example, in pilot runs discriminating among SOD metallo-forms we found that pico-prasinophytes encode Mn-SOD instead of the Fe-SOD encoded in genomes from larger green algal phytoplankters (Data not visualized) [133].

With increasing cell radius, eukaryotic phytoplankton have a smaller fraction of their total genes encoding scavenging of $O_2^{\bullet-}$ (Fig 3, Blue line, Slope = $-2.1\times10^{-1} \pm 7.1\times10^{-2}$, p-value = 4.2×10^{-3}, pseudo-R^2 = 0.087). The negative slope does not support our Hypothesis 1 that phytoplankton do not differentially allocate a changing fraction of their total gene content to $O_2^{\bullet-}$ scavenging with increasing cell size. Including 'Flagella' and 'Colony' as co-variates in the regression results, however, in a slope that is not statistically different from zero (Fig 3, Black line, Slope = $-6.7\times10^{-2} \pm 6.8\times10^{-2}$, p-value = 3.3×10^{-1}), driven by the influence of 'Flagella' (p-value = 3.7×10^{-2}) but not 'Colony' (p-value = 8.6×10^{-1}). $O_2^{\bullet-}$ metabolism in phytoplankton appears to be mediated by a nearly fixed set of core genes that do not change with increasing total gene count, thus the fractional gene allocation to $O_2^{\bullet-}$ decreases as cell radius, and the co-varying total gene count increases. Therefore, gene dosage does not emerge as a factor in phytoplankton $O_2^{\bullet-}$ metabolism. With increasing cell radius, eukaryotic phytoplankton have no cell-size associated difference in genes encoding superoxide scavenging, when normalized to total ribosomal genes, suggesting that as a fraction of housekeeping genes, cells do not increase their genomic capacity to scavenge superoxide, consistent with our hypothesis 1 (Data not visualized, Slope = $-2.4\times10^{-1} \pm 2.5\times10^{-1}$, p-value = 3.3×10^{-1}).

Consistent with the significant influence of flagella on the regressions vs. median cell radius (Fig 3), flagellated phytoplankton, irrespective of size, have a smaller proportion of their total gene content encoding $O_2^{\bullet-}$ scavenging (Fig 4, p-value = 4.3×10^{-3}), than do non-flagellated phytoplankton. Similarly, irrespective of size, flagellated phytoplankton have a smaller ratio of genes encoding $O_2^{\bullet-}$ scavenging to their total ribosomal genes (Data not visualized, p-value = 3.2×10^{-10}). This suggests that cellular motility contributes to phytoplankton homeostasis of $O_2^{\bullet-}$, possibly by supporting escape from localized extracellular pockets of $O_2^{\bullet-}$. This decrease in proportional allocation to $O_2^{\bullet-}$ scavenging is also arithmetically consistent with the difference in the number of total genes between flagellated and non-flagellated phytoplankton, whereby flagellated phytoplankton have more total genes.

Pennate and centric diatoms have similar fractions of their genomes encoding $O_2^{\bullet-}$ scavenging (p-value = 9.7×10^{-1}), as well as similar ratios of $O_2^{\bullet-}$ scavenging genes to their housekeeping ribosomal genes (p-value = 8.1×10^{-1}) (Data not visualized). Our results support our hypothesis that differential diffusional exchange across diatoms of different shape does not influence the fraction of total gene content encoding $O_2^{\bullet-}$ scavenging enzymes, because $O_2^{\bullet-}$

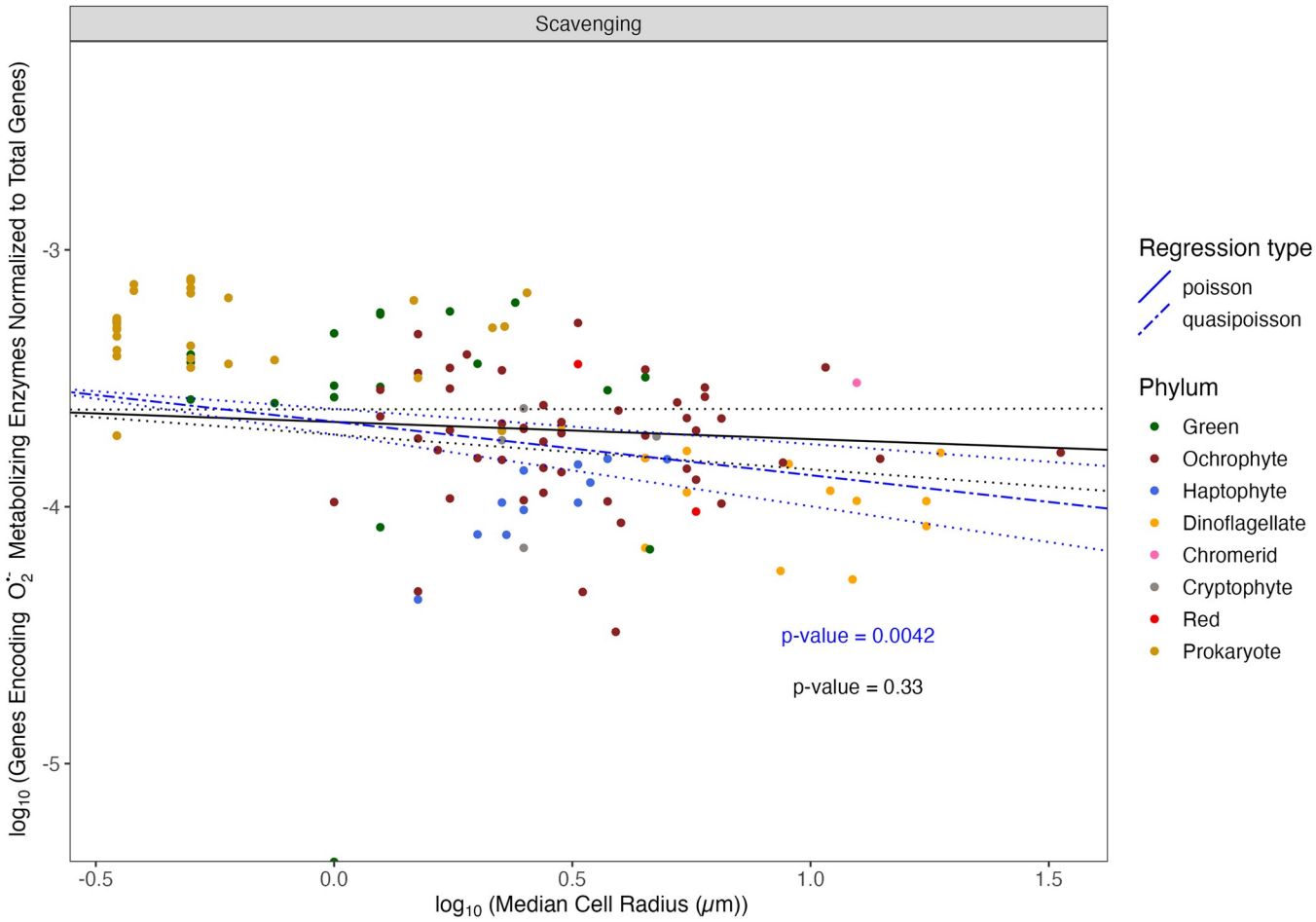

Fig 3. Comparison of log_{10} (Total number of genes encoding O2•− metabolizing enzymes ('SupOx_count') normalized to the total number of genes present in each organism ('GeneModels_count')) vs. the log_{10} (median cell radius in μm ('log_Radius_um')). Poisson (solid line) or Quasi-Poisson (dashed line) regressions fitted to data ± Standard Error (dotted line). Regressions were run with (black line) or without (blue line) 'Colony' and 'Flagella' as co-variates. Selected prokaryote genomes are presented for comparison, but excluded from the presented regressions. Symbol color corresponds to taxon lineage ('Phylum').

https://doi.org/10.1371/journal.pone.0284580.g003

diffusion outwards is limited by the cell membrane, regardless of cell shape (Hypothesis 1). Differences between genomic patterns of pennate and centric diatoms may arise when comparing metallo-forms of SOD, noting that [145] found that pennate diatoms transcribe Cu/Zn-SOD but not Fe-SOD, whereas centric diatoms transcribe Fe-SOD more frequently than they transcribe Cu/Zn-SOD.

Hydrogen peroxide

All prokaryotic (S9 Fig) and eukaryotic (S10 Fig) phytoplankton, with the exception of a single transcriptome from the prasinophyte *Micromonas polaris*, have genes encoding H_2O_2 producing enzymes, as they all carry gene(s) encoding the ubiquitous enzyme Superoxide Dismutase. Genes encoding oxidases producing H_2O_2 include copropophyrinogen oxidase, found across all eukaryotic and prokaryotic phytoplankton, with the exception of one transcriptome. Genes encoding thiol oxidase and acyl CoA oxidase are also found in nearly all eukaryotic phytoplankton, with the exceptions of three transcriptomes. Genes encoding L-aspartate oxidase are found in nearly all prokaryotes, and all green algae, but are nearly absent from other eukaryotic

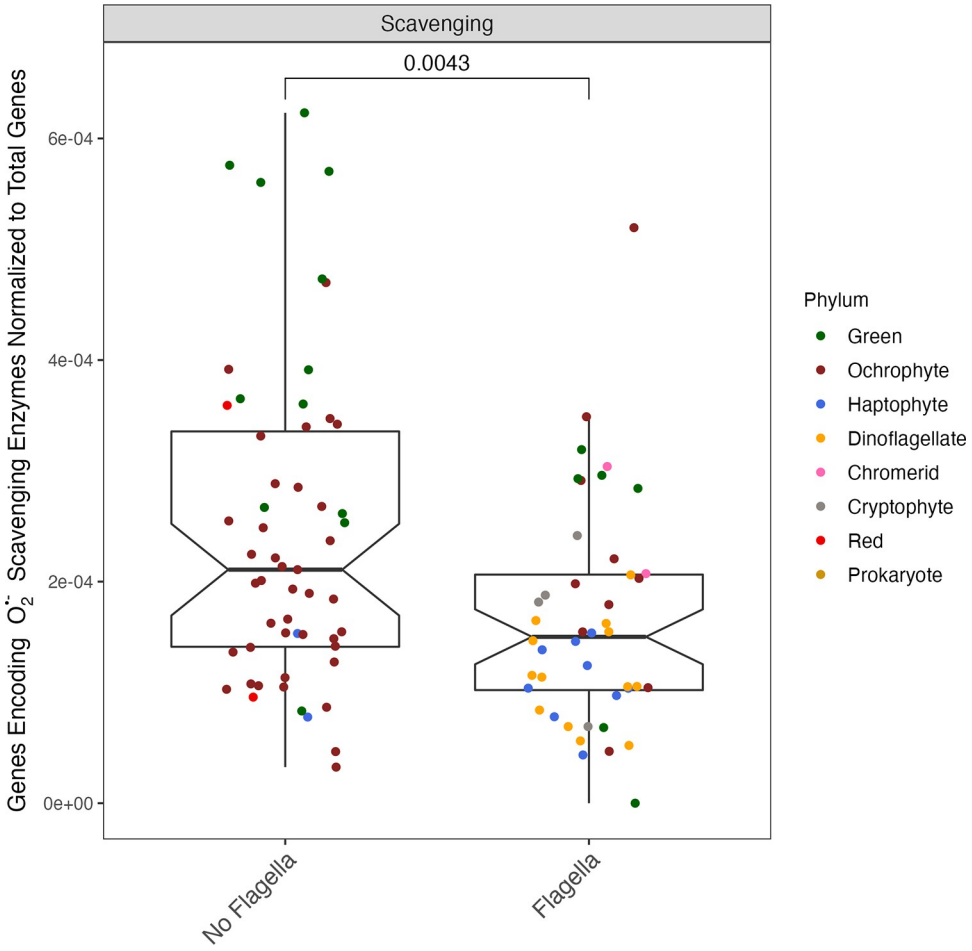

Fig 4. Comparison of total number of genes encoding O2•− scavenging enzymes ('SupOx_count') normalized to the total number of genes present in each organism ('GeneModels_count')) vs. the presence or absence of flagella in the organism. Symbol color corresponds to taxon lineage ('Phylum'). Notch spans ± standard error of the median. Box spans median ± 1 quartile of the data. Whiskers span the range excluding outliers in the data. Citations for data sources can be found in S3 Table.

https://doi.org/10.1371/journal.pone.0284580.g004

taxa. Sarcosine oxidase is not present in small diatoms and small green algae, but is present in nearly all dinoflagellates and haptophytes. (S)-2-hydroxy-acid oxidase (whose EC number includes glycolate oxidase) is found in most eukaryotic phytoplankton, but rarely in dinoflagellates.

Most prokaryotic phytoplankton (S9 Fig) and all eukaryotic (S10 Fig), have genes encoding H_2O_2 scavenging enzymes. Some strains of *Prochlorococcus* and *Synechococcus* have lost all genomic capacity to scavenge H_2O_2, and appear to rely on co-occurring hosts for H_2O_2 scavenging [83, 84, 87].

The absence of catalase from most analyzed cyanobacterial genomes supports [146] who analyzed 44 different cyanobacterial genomes and found that only *Nostoc punctiforme* PCC73102 retained a full gene encoding catalase. In our analyses, only *Synechococcus elongatus* PCC11802 maintained a catalase encoding gene (S9 Fig). In the greens, catalase has been lost from the smaller prasinophytes but is maintained in the larger greens (S10 Fig). The loss of catalase from smaller green algae may be evidence of the Black Queen Hypothesis in action [83], in that H_2O_2 can passively diffuse out of the smaller green algae but diffuses less out of larger

green algae. Loss of function mutations in catalase encoding genes in small algae are therefore less deleterious than they would be to large green algae. Catalase, with a K_M of ~220 mM, may be poorly retained because the cells maintain some genomic capacity to scavenge H_2O_2 using the enzymes ascorbate peroxidase, glutathione peroxidase and Cytochrome C peroxidase (S10 Fig), with K_M in the low μM range [146].

Our results support an earlier suggestion that bigger genomic capacity for H_2O_2 scavenging in *Synechococcus* compared to *Prochlorococcus* is a result of the larger size in *Synechococcus* compared to *Prochlorococcus* [84] (S9 Fig). It is however important to note the vast differences between prokaryotic and eukaryotic phytoplankton, with most eukaryotic phytoplankton, regardless of lineage, maintaining the genomic capacity to produce ascorbate peroxidase, glutathione peroxidase and Cytochrome C peroxidase (S10 Fig). Peroxidases are involved in pathways beyond simple ROS scavenging, including the Halliwell-Asada cycle for ascorbate peroxidase [147]. *Ostreococcus*, the smallest prasinophyte has a radius of 0.5 μm, comparable to that of the prokaryote *Synechococcus* (S3 Table), and would therefore share a similarly short diffusion path length. Nevertheless *Ostreococcus*, in common with other eukaryotes, retains genomic capacities to produce ascorbate peroxidase, glutathione peroxidase and cytochrome c peroxidase, which may thus reflect the cost of being eukaryotic (S10 Fig).

With increasing cell radius, eukaryotic phytoplankton have a smaller fraction of their total genes encoding the production of H_2O_2 (Fig 5, Blue line, Slope = $-3.4\times10^{-1} \pm 5\times10^{-2}$, p-value = 9.6×10^{-10}, pseudo-R^2 = 0.34). Including 'Flagella' and 'Colony' as co-variates did not significantly alter this pattern (Black line, 'Flagella' p-value = 8.4×10^{-1}, 'Colony' p-value = 4.7×10^{-1}). The pattern of a smaller fraction of total genes for H_2O_2 production with increasing cell radius supports our Hypothesis 2 that larger phytoplankton counter decreasing diffusional loss of H_2O_2 out of cells through a lower genomic capacity for H_2O_2 production, whereas losses of genes encoding H_2O_2 producing enzymes are more costly to small phytoplankton (Fig 5). [7] found that a major influence upon the capacity for production of H_2O_2 is whether or not the organism can form blooms, with bloom forming species producing more H_2O_2. The ability to form blooms was not analyzed in our data as we did not find systematic information on potentials for bloom formation across taxa.

With increasing cell radius, eukaryotic phytoplankton also have a smaller fraction of their total genes encoding the capacity to scavenge H_2O_2 (Fig 5, Blue line, Slope = $-3.2\times10^{-1} \pm 5.6\times10^{-2}$, p-value = 1.4×10^{-7}, pseudo-R^2 = 0.26). Including 'Flagella' and 'Colony' as co-variates did not influence the negative slope of the fraction of total genes encoding H_2O_2 scavenging with increasing median cell radius (Fig 5, Black line, 'Flagella' p-value = 4.1×10^{-1}, 'Colony' p-value = 1.6×10^{-1}). A parallel analysis focusing only on small phytoplankton such as pico-cyanobacteria and pico-prasinophytes might yield different results as more such genomes are sequenced, since [148] found that H_2O_2 added to seawater at a concentration of 1.6 mg L^{-1} did not affect cells with a radius larger than 1 to 1.5 μm, but differentially harmed the picoprasinophyte *Micromonas pusilla*.

Because median cell radius co-varied with Taxa, we generally excluded Taxa as a co-variate from our regressions, in order to focus on any cross-taxon patterns driven by changing median cell radius. Nevertheless, representatives of the Ochrophyte Phylum alone spanned more than an order of magnitude in median cell radius. We therefore tested whether the $\log_{10}$(total number of genes encoding the metabolism of $O_2^{\bullet-}$, H_2O_2 or $^{\bullet}NO$) varied with the $\log_{10}$ (median cell radius) across the Ochrophytes alone (S7 Fig). We found that across Ochrophytes, the fraction of total genes encoding the production of H_2O_2 decreased with increasing cell radius (Slope = $-1.6\times10^{-1} \pm 9.4\times10^{-2}$), although the p-value for the regression was only 1×10^{-1}). This marginal decrease in the total number of genes encoding H_2O_2 production with increasing median cell radius in Ochrophytes again tends to support our Hypothesis 2, with data from

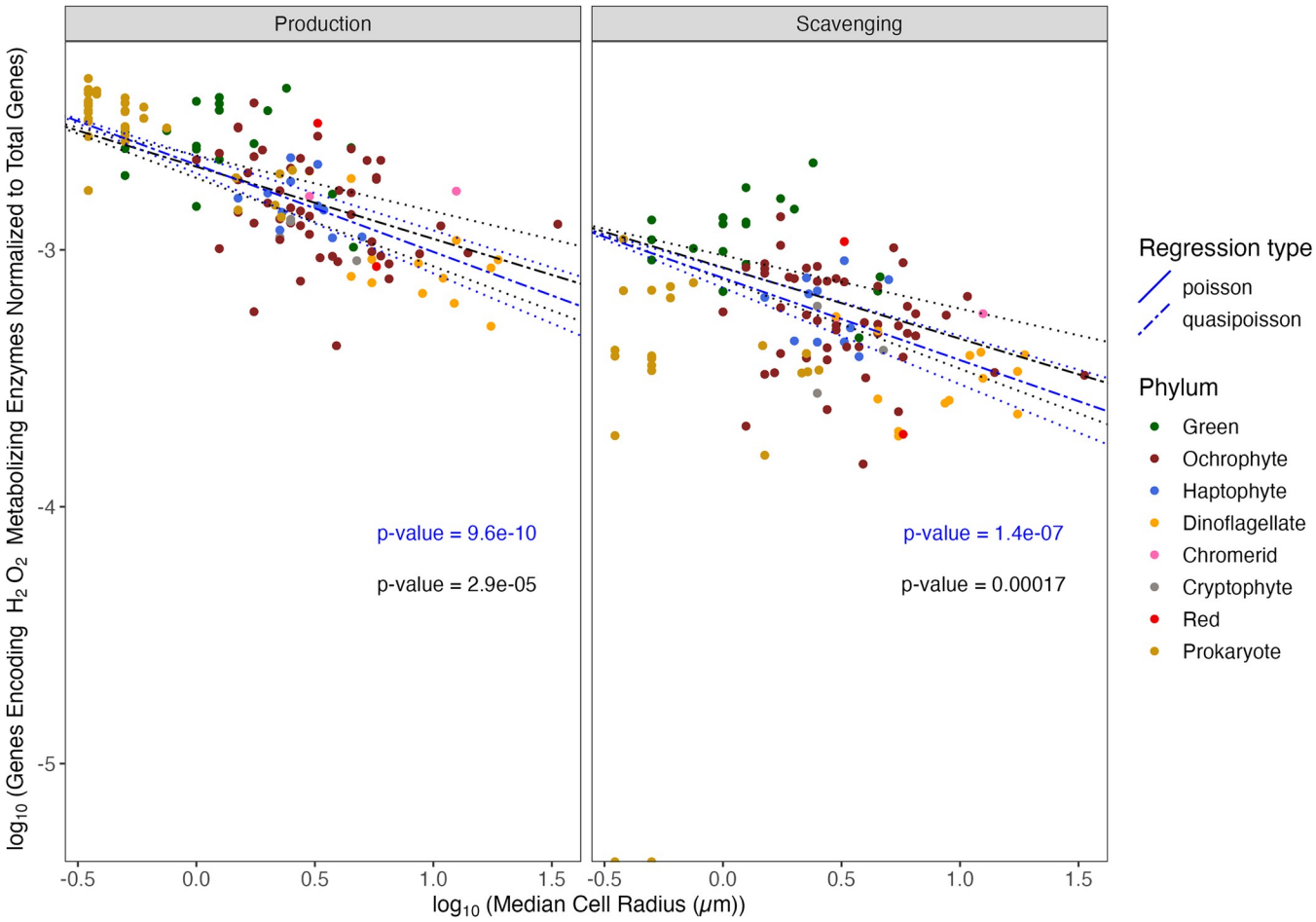

Fig 5. Comparison of $\log_{10}$ (Total number of genes encoding H_2O_2 metabolizing enzymes ('HyPe_count') normalized to the total number of genes present in each organism ('GeneModels_count')) vs. the $\log_{10}$ (median cell radius in μm ('log_Radius_um')). Poisson (solid line) or Quasi-Poisson (dashed line) regressions fitted to data ± Standard Error (dotted line). Regressions were run with (black line) or without (blue line) 'Colony' and 'Flagella' as co-variates. Selected prokaryote genomes are presented for comparison, but excluded from the presented regressions. Symbol color corresponds to taxon lineage ('Phylum'). Citations for data sources are in S3 Table.

https://doi.org/10.1371/journal.pone.0284580.g005

within a single phylum to limit confounding influences of diverse evolutionary histories and cell biologies upon patterns.

H_2O_2 production (Slope = $-3.7\times10^{-1} \pm 2\times10^{-1}$, p-value = 6.7×10^{-2}) and scavenging (Slope = $-3.5\times10^{-1} \pm 2.1\times10^{-1}$, p-value = 1×10^{-1}) allocations were steady with increasing cell size, relative to the ribosomal housekeeping gene proxy. But, genes for H_2O_2 production and scavenging are diluted by increasing total gene counts with increasing cell size.

Pennate and centric diatoms do not show statistically significant differences in the fraction of their total gene content encoding the production (p-value = 1.9×10^{-1}) nor the scavenging of H_2O_2 (p-value = 9.6×10^{-2}). Pennate and centric diatoms also do not show statistically significant differences in the ratio of genes encoding production (p-value = 3.3×10^{-1}) nor the scavenging of H_2O_2 (p-value = 3.9×10^{-1}), normalized to their ribosomal gene content encoding H_2O_2. These results do not support our Hypothesis 5 that pennates have more genes encoding H_2O_2 producing enzymes due to their higher surface area to volume ratio (Data not visualized).

Nitric oxide

In the genomes and transcriptomes that we analysed, Nitric Oxide Synthase (NOS, EC:1.14.13.39), although often absent, was the most frequently occurring •NO producing enzyme encoded (S11 Fig), but was not encoded, or at least not annotated, among prokaryotic phytoplankton (Data not visualized).

Nitric Oxide Dioxygenase (NOD, EC:1.14.12.17) was the most frequently occurring of the •NO scavenging enzymes (S11 Fig). NOD sequences were identified in some eukaryotes, but were either not annotated, or not present in *Prochlorococcus*, most green algae and most centric diatoms. A NOS-like sequence that also has Nitric Oxide Dioxygenase-like function [149] has recently been identified in *Synechococcus*, which might encode NOD activity in some strains lacking annotated NOD sequences.

With increasing cell radius eukaryotic phytoplankton do not vary in the fraction of total genes encoding the capacity to produce •NO (Fig 6, Blue line, Slope = $-2.5\times10^{-1} \pm 1.7\times10^{-1}$, p-value = 1.5×10^{-1}). We re-ran the Quasi-Poisson, excluding those phytoplankton that completely lack genes encoding enzymes for •NO production (NitOx_count = 0, points along

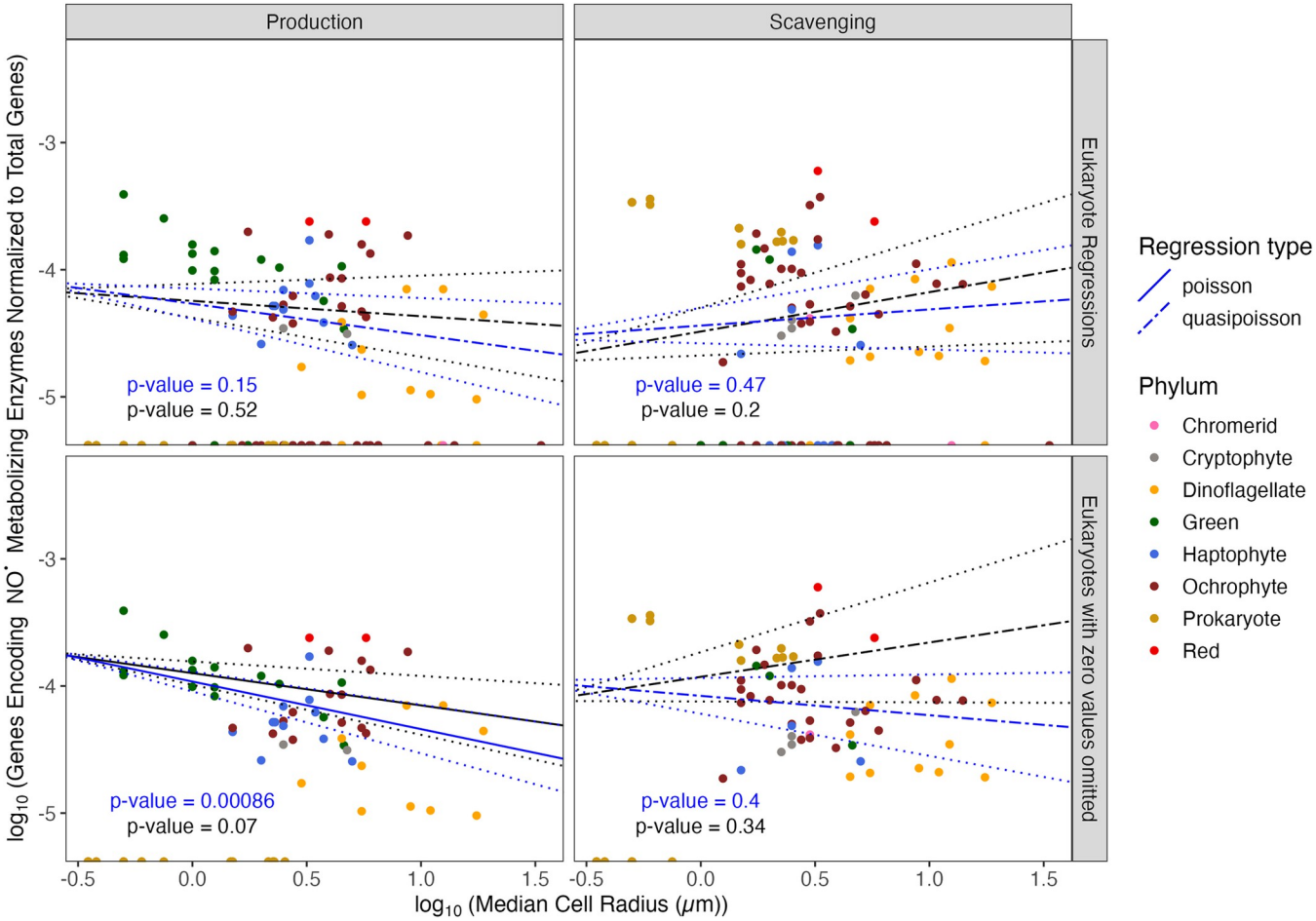

Fig 6. Comparison of $\log_{10}$ (Total number of genes encoding •NO metabolizing enzymes ('NitOx_count') normalized to the total number of genes present in each organism ('GeneModels_count')) vs. the $\log_{10}$ (median cell radius in μm ('log_Radius_um')). Poisson (solid line) or Quasi-Poisson (dashed line) regressions fitted to data ± Standard Error (dotted line). Regressions were run with (black line) or without (blue line) 'Colony' and 'Flagella' as co-variates. Selected prokaryote genomes are presented for comparison, but excluded from the presented regressions. Symbol color corresponds to taxon lineage ('Phylum').

https://doi.org/10.1371/journal.pone.0284580.g006

the x-axis), which resulted in a decreasing slope with increasing cell radius. Thus, those phytoplankton with any detected capacity to produce •NO indeed have a smaller fraction of their total genes encoding •NO production with increasing radius (Fig 6, Blue line, Slope = $-3.7\times10^{-1} \pm 1.1\times10^{-1}$, p-value = 8.6×10^{-4}, pseudo-R^2 = 0.13). Including 'Flagella' and 'Colony' as co-factors for the regression that solely looks at phytoplankton with the genomic capacity to produce •NO resulted in a slope that is no longer significantly different from zero (Fig 6, Black line, Slope = $-2.5\times10^{-1} \pm 1.4\times10^{-1}$, p-value = 7×10^{-2}), driven by the influence of 'Flagella' (p-value = 1.4×10^{-4}), but not 'Colony' (p-value = 1.8×10^{-1}).

With increasing cell radius, eukaryotic phytoplankton do not vary in the fraction of their total genes encoding the capacity to scavenge •NO, Quasi-Poisson regression slope not significantly different from zero (Fig 6, Blue line, Slope = $1.3\times10^{-1} \pm 1.8\times10^{-1}$, p-value = 4.7×10^{-1}).

Non-enzymatic paths contribute to intracellular and extracellular •NO production [150], and may explain the absences of genes encoding •NO production from some genomes across taxonomic lineages. Alternately, •NO homeostasis may be achieved in some lineages by regulating the active cellular uptake and release of intracellular •NO, as has been recently demonstrated in humans [151]. Although NOD sequences have only been identified from phytoplankton through meta-transcriptomic analyses, in diatoms, haptophytes and dinoflagellates [152], there is limited understanding as to what may contribute to the active removal of •NO, and the lack of •NO scavenging genes across multiple phytoplankters. More research is needed on possible contributions of NOD to the active removal of •NO, as well as the NOS sequences detected in *Synechococcus* that also display NOD-like activity [149]. Perhaps the low toxicity of •NO does not warrant the active removal of •NO as long as the concentration does not exceed the toxic threshold. This explanation is plausible given that *Platymonas helgolandica*, *Platymonas subcordiformis*, *Skeletonema costatum*, *Gymnodinium* sp., and *Prorocentrum donghaiense* showed optimum growth in the presence of •NO concentrations between 10^{-9} and 10^{-6} mol L^{-1} [153], which are higher than the concentrations found in the ocean (Table 1).

A binomial model comparing the presence or absence of genes that encode the production of •NO shows no cell size effect (slope = -3.5×10^{-1}, p = 1.4×10^{-1}). Including 'Flagella' as a co-variate does not alter these results, but does show that flagellated phytoplankton have higher likelihood of presence of •NO production than do non-flagellated phytoplankton (S12 Fig, p = 5.6×10^{-5}). Including 'Colony' as a co-variate does not show a cell size effect, nor a difference in the likelihood of •NO production between colony and non-colony forming phytoplankton (p = 1.3×10^{-1}).

In contrast, larger phytoplankton are more likely to have a gene encoding •NO scavenging (slope = 1.1×10^{0}, p = 2×10^{-4}). This trend is not influenced by flagella (p = 1.9×10^{-1}) nor colony formation (p = 1.3×10^{-1}). This pattern supports our hypothesis that larger, diffusionally limited cells, have a stronger requirement for •NO scavenging (Hypothesis 2).

Most centric diatoms carry genes annotated as encoding •NO producing enzymes, whereas most pennate diatoms do not (p-value = 6.2×10^{-3}) when normalized to total genes, and when normalized to ribosomal genes (p-value = 1.1×10^{-2}). In contrast, most centric diatoms lack genes annotated as encoding •NO scavenging enzymes, whereas most pennate diatoms carry those genes (p-value = 3.8×10^{-5}) when normalized to total genes, and p-value = 2.4×10^{-5} when normalized to ribosomal genes) (Fig 7).

The larger fractional gene allocation to •NO production, and smaller fraction of genes that encode •NO scavenging enzymes, in centric diatoms (Fig 7) counters our hypothesis that diffusion from pennate diatoms would drive gene allocations in favor of •NO production (Hypothesis 5). Given the strong contrast in annotated •NO metabolism genes, it is likely that •NO has regulatory or signaling roles that vary systematically between pennate and centric diatoms, outside any diffusional influences. For example, •NO inhibits diatom adhesion to substrate

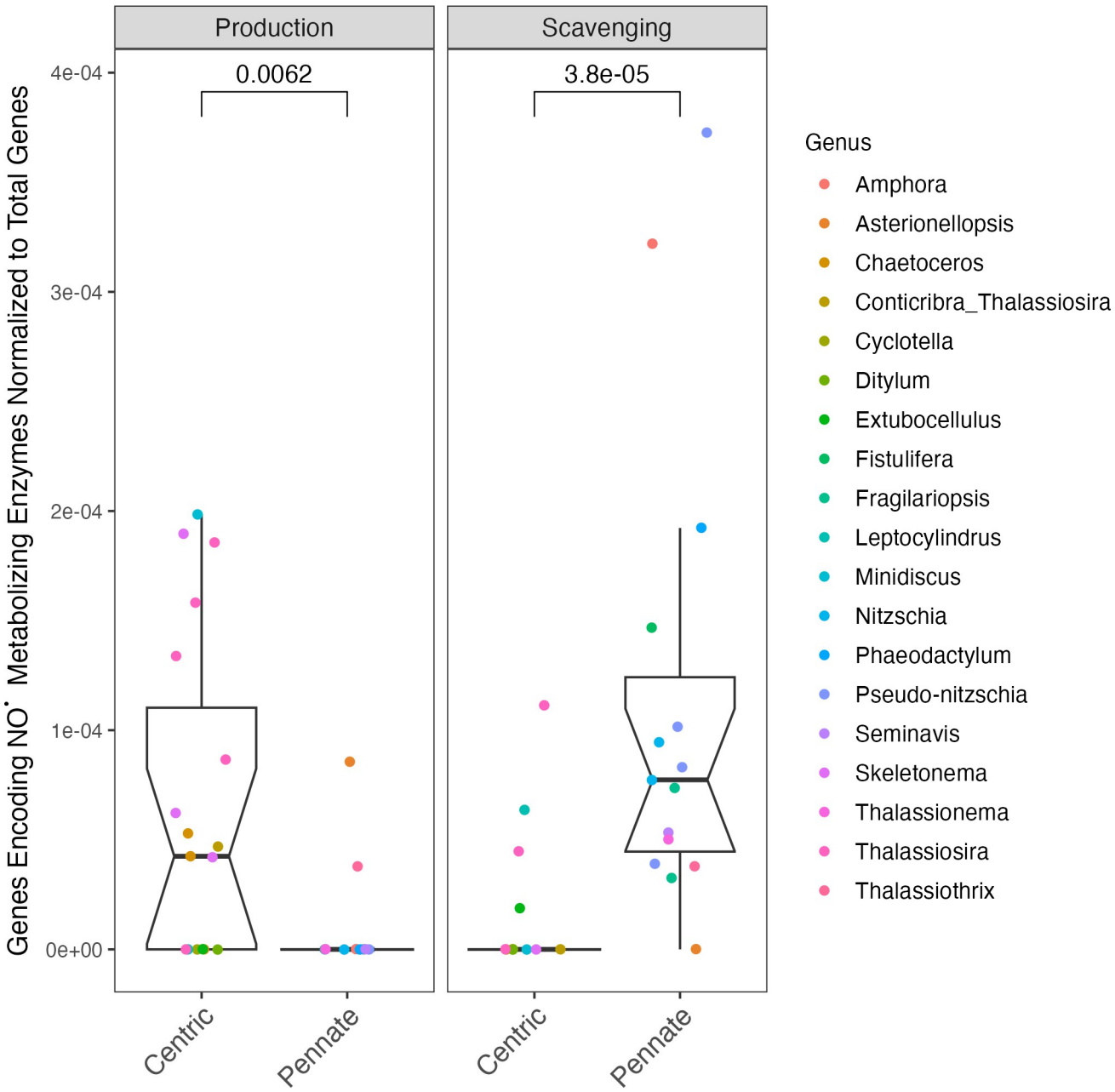

Fig 7. Comparison of total number of genes encoding •NO metabolizing enzymes ('NitOx_count') normalized to the total number of genes present in each diatom ('GeneModels_count') vs. the growth form of the diatom ('PennateCentric'). Symbol color corresponds to taxon lineage ('Phylum'). Notch spans ± standard error of the median. Box spans median ± 1 quartile of the data. Whiskers span the range excluding outliers in the data. Citations for data sources can be found in S3 Table.

https://doi.org/10.1371/journal.pone.0284580.g007

[72, 154]. Pennates are more likely to grow adhered in biofilms [155], which may explain the striking differences in total gene allocation to •NO production and scavenging. Alternately, [156] identified putative NOS sequences in the transcriptomes of three pennate diatom species (*Pseudo-nitzschia arenysensis*, *Pseudo-nitzschia delicatissima* and *Pseudo-nitzschia multi-striata*), so it is possible the apparent lack of •NO producing sequences in pennates is due to errors in the unsupervised annotations from eggNOG.

Summary

We analyzed the fractions of the total genes in the genome that are associated with the metabolisms of three major ROS. It is important to note that the content of genes encoding specific ROS metabolizing enzymes may be caused by genetic drift, or may relate to a selective advantage linked to other metabolites of the same enzymes, rather than an enzyme role in ROS metabolism, *per se*. Furthermore, the gene presence or gene count in a genome is only one influence on the potential activity of the encoded enzyme, and closely related enzymes may confer different activities in different organisms.

The differential reactivities, diffusion distances, diffusibilities across cell membranes, and roles in cell signaling of H_2O_2, $O_2^{\bullet-}$ and $^{\bullet}NO$ (Table 1) influence genomic allocation patterns for the production and scavenging of these three distinct ROS.

$O_2^{\bullet-}$ has high reactivity, short intracellular and extracellular lifetimes and limited cell membrane crossing. We did not find genes specifically encoding $O_2^{\bullet-}$ production in eukaryotic phytoplankton genomes. As expected, genes encoding $O_2^{\bullet-}$ scavenging were ubiquitous, but the fractional gene allocation to $O_2^{\bullet-}$ scavenging decreases as cell radius, and the co-varying total gene count increases, consistent with a nearly fixed set of core genes scavenging $O_2^{\bullet-}$ that do not change with increasing gene count in larger cells (Hypothesis 1).

H_2O_2 has lower reactivity, longer intracellular and extracellular lifetimes and readily crosses cell membranes. Across eukaryotic phytoplankton, the fraction of the total genes encoding H_2O_2 producing and scavenging enzymes decreases with increasing cell radius (partially supports hypothesis 5). Presence of flagella and colony formation do not appear to influence H_2O_2 metabolism (contrary to hypotheses 3 & 4)

$^{\bullet}NO$ has low reactivity, long intracellular and extracellular lifetimes and readily crosses cell membranes. Neither the fraction of the total genes for $^{\bullet}NO$ production nor for scavenging changed significantly with increasing cell radius, consistent with relatively low cytotoxicity and roles of $^{\bullet}NO$ in taxonomically diverse regulatory systems (contrary to hypothesis 5). Pennate diatoms frequently lack genes annotated as encoding $^{\bullet}NO$ producing enzymes, whereas centric diatoms frequently lack genes annotated as encoding $^{\bullet}NO$ scavenging enzymes (contrary to hypothesis 5). This finding is not explicable by differential diffusional losses of $^{\bullet}NO$, but may reflect distinct roles of $^{\bullet}NO$ in the regulatory systems of diatom lineages.

Supporting information

S1 Fig. Violin plot presenting the range of $\log_{10}$ of the median cell radius in μm ('log_Radius_um') for each taxonomic lineage ('Phylum'). Point colour corresponds to the source of the data, whether Genome or Transcriptome ('Ome'). Violin width indicates the fraction of all datapoints occurring at a cell radius ('log_Radius_um') within a phylum. Citations for data sources are in S3 Table.
(TIF)

S2 Fig. Longitude and latitude of isolation of analyzed organisms, overlaid on a world map Point colour corresponds to the taxonomic lineage ('Phylum'). Ocean colour corresponds to depth Citations for data sources are in S3 Table. Data used to generate world map produced from the 'ggOceanMaps' R package [157].
(TIF)

S3 Fig. Comparison of paired counts of particular genes encoding ROS production or scavenging from the genome ('ROSGene_count.g') or transcriptome ('ROSGene_count.t') taken from the same organism. Data was drawn from a subset of analyzed organisms for which both genome and transcriptome were available. Colour corresponds to the taxonomic

lineage ('Phylum') Points are jittered to avoid overlapping, resulting in blocks around frequently occurring counts. Dashed line is at 1:1 where 'ROSGene_count.g' and 'ROSGene_count.t' would be equal. Citations for data sources are in S3 Table.
(TIF)

S4 Fig. Comparison of paired counts of particular genes encoding ROS production or scavenging from manual and automatic annotations taken from the same organism. Data was drawn from a subset of genomes and transcriptomes which were both manually and automatically annotated. Colour corresponds to the 'Gene' Points are jittered to avoid overlapping, resulting in blocks around frequently occurring counts. Dashed line is placed at 1:1 where Manual and Automated counts would be equal. Citations for data sources in S4 Table.
(TIF)

S5 Fig. Histogram of occurrences of number of total genes, in a genome or transcriptome, (y axis) that code for the production of enzymes that produce or scavenge H_2O_2, O2•− or •NO in vivo. Symbol color corresponds to taxon lineage ('Taxa').
(TIF)

S6 Fig. Comparison of $\log_{10}$ of the total number of ribosomal genes in an organism ('log10 (RibosomeCount)') to $\log_{10}$ of the median cell radius in μm ('log_Radius_um'). Colour corresponds to the taxonomic lineage ('Phylum'), whereas symbol shape corresponds to the source of the data, whether Genome or Transcriptome ('Ome'). Citations for data sources are in S3 Table.
(TIF)

S7 Fig. Comparison of $\log_{10}$ (Total number of genes encoding H_2O_2, O2•− or •NO metabolizing enzymes normalized to the total number of genes present in each Ochrophyte) vs. the $\log_{10}$(median cell radius in μm). Poisson (solid line) or Quasi-Poisson (dashed line) regressions fitted to data ± Standard Error (dotted line). Regressions were run without (blue line) 'Colony' and 'Flagella' as co-variates. Citations for data sources are in S3 Table.
(TIF)

S8 Fig. Summary of O2•− scavenging enzymes encoded within genomes and transcriptomes of eukaryotic phytoplankton analyzedTaxa are ordered from top to bottom along the left according to increasing median cell diameter within each taxonomic lineage. Symbol colour corresponds to taxonomic lineages ('Taxa'). Filled data points indicate that the data obtained from that organism was sourced from a genome, and unfilled data points were sourced from a transcriptome. The size of the symbol increases with the number of members of each enzyme found within each genome or transcriptome. Symbol absence means no sequences known to encode the enzyme family of interest were found in the target genome or transcriptome. The absence of transcripts encoding SOD from the Micromonas polaris transcriptome is likely due to low expression of SOD at the time that the mRNA was harvested for sequence analyses.
(TIF)

S9 Fig. Summary of H_2O_2 metabolizing enzymes encoded within genomes of prokaryotic phytoplankton analyzed, faceted by whether the enzymes produce or scavenge H_2O_2. Taxa are ordered from top to bottom along the left according to increasing median cell diameter within each taxonomic lineage. Symbol colour corresponds to the genus of the prokaryote. Filled data points indicate that the data obtained from that organism was sourced from a genome. The size of the symbol increases with the number of members of each enzyme found within each genome or transcriptome. Symbol absence means no sequences known to encode

the enzyme family of interest were found in the target genome or transcriptome.
(TIF)

S10 Fig. Summary of H_2O_2 metabolizing enzymes encoded within genomes and transcriptomes of eukaryotic phytoplankton analyzed, faceted by whether the enzymes produce or scavenge H_2O_2. Taxa are ordered from top to bottom along the left according to increasing median cell diameter within each taxonomic lineage. Symbol colour corresponds to taxonomic lineages ('Taxa'). Filled data points indicate that the data obtained from that organism was sourced from a genome, and unfilled data points were sourced from a transcriptome. The size of the symbol increases with the number of members of each enzyme found within each genome or transcriptome. Symbol absence means no sequences known to encode the enzyme family of interest were found in the target genome or transcriptome.
(TIF)

S11 Fig. Summary of $^{\bullet}NO$ metabolizing enzymes encoded within genomes and transcriptomes of eukaryotic phytoplankton analyzed, faceted by whether the enzymes produce or scavenge $^{\bullet}NO$. Taxa are ordered from top to bottom along the left according to increasing median cell diameter within each taxonomic lineage. Symbol colour corresponds to taxonomic lineages ('Taxa'). Filled data points indicate that the data obtained from that organism was sourced from a genome, and unfilled data points were sourced from a transcriptome. The size of the symbol increases with the number of members of each enzyme found within each genome or transcriptome. Symbol absence means no sequences known to encode the enzyme family of interest were found in the target genome or transcriptome.
(TIF)

S12 Fig. Comparison of the probability of having the genomic capacity to encode $^{\bullet}NO$ vs. the $\log_{10}$ (median cell radius in μm ('log_Radius_um')). Colony (solid line) or non-colony (dashed line) regressions fitted to data. Points along the y-axis indicate whether an organism has flagella (1) or does not have flagella (0).
(TIF)

S1 Table. Variable names, definitions, units, and first location of occurrence in code, used for our data.
(CSV)

S2 Table. Enzyme commission number, kegg orthology number, enzyme name and ROS substrate metabolized.
(CSV)

S3 Table. Metadata for each organism.
(CSV)

S4 Table. Comparison of manual and automated gene counts.
(CSV)

S1 File. References for S1 to S4 Tables.
(DOCX)

Acknowledgments

The authors would like to thank Dr. Marek Eliáš and Dr. Zoltán Füssy for their advice with the initial methodology, Dr. Maximilian Berthold for his assistance in coding and for his comments, Dr J. Scott McCain and Dr. Irena Kaczmarska for comments. Some sequences were

accessed from The Marine Microbial Eukaryotic Transcriptome Sequencing Project (MMETSP) supported by the Gordon and Betty Moore Foundation through a grant to the National Center for Genome Resources.

Author Contributions

Conceptualization: Naaman M. Omar, Katherine Fleury, Ondřej Prášil, Douglas A. Campbell.

Data curation: Naaman M. Omar, Katherine Fleury, Brian Beardsall, Douglas A. Campbell.

Funding acquisition: Douglas A. Campbell.

Investigation: Naaman M. Omar.

Methodology: Naaman M. Omar, Katherine Fleury, Brian Beardsall, Douglas A. Campbell.

Supervision: Douglas A. Campbell.

Validation: Katherine Fleury, Douglas A. Campbell.

Visualization: Naaman M. Omar, Katherine Fleury.

Writing – original draft: Naaman M. Omar, Katherine Fleury, Douglas A. Campbell.

Writing – review & editing: Naaman M. Omar, Katherine Fleury, Brian Beardsall, Ondřej Prášil, Douglas A. Campbell.

References

1. Finkel ZV, Beardall J, Flynn KJ, Quigg A, Rees TAV, Raven JA. Phytoplankton in a changing world: Cell size and elemental stoichiometry. J Plankton Res. 2010; 32: 119–137. https://doi.org/10.1093/plankt/fbp098
2. Andersen KH, Aksnes DL, Berge T, Fiksen Ø, Visser A. Modelling emergent trophic strategies in plankton. J Plankton Res. 2015; 37: 862–868. https://doi.org/10.1093/plankt/fbv054
3. Finkel ZV. Light absorption and size scaling of light-limited metabolism in marine diatoms. Limnol Oceanogr. 2001; 46: 86–94. https://doi.org/10.4319/lo.2001.46.1.0086
4. Geider R, Piatt T, Raven J. Size dependence of growth and photosynthesis in diatoms: A synthesis. Mar Ecol Prog Ser. 1986; 30: 93–104. https://doi.org/10.3354/meps030093
5. Strom SL, Macri EL, Olson MB. Microzooplankton grazing in the coastal Gulf of Alaska: Variations in top-down control of phytoplankton. Limnol Oceanogr. 2007; 52: 1480–1494. https://doi.org/10.4319/lo.2007.52.4.1480
6. Litchman E, de Tezanos Pinto P, Klausmeier CA, Thomas MK, Yoshiyama K. Linking traits to species diversity and community structure in phytoplankton. In: Naselli-Flores L, Rossetti G, editors. Fifty years after the "Homage to Santa Rosalia": Old and new paradigms on biodiversity in aquatic ecosystems. Dordrecht: Springer Netherlands; 2010. pp. 15–28. https://doi.org/10.1007/978-90-481-9908-2_3
7. Diaz JM, Plummer S. Production of extracellular reactive oxygen species by phytoplankton: Past and future directions. J Plankton Res. 2018; 40: 655–666. https://doi.org/10.1093/plankt/fby039 PMID: 30487658
8. Schneider R. Kinetics of Biological Hydrogen Peroxide Production. Doctor of {{Philosophy}} ({{Geochemistry}}), Colorado School of Mines. 2015.
9. Lesser MP. Oxidative Stress in Marine Environments: Biochemistry and Physiological Ecology. Annu Rev Physiol. 2006; 68: 253–278. https://doi.org/10.1146/annurev.physiol.68.040104.110001 PMID: 16460273
10. Bienert GP, Chaumont F. Aquaporin-facilitated transmembrane diffusion of hydrogen peroxide. Biochim Biophys Acta. 2014; 1840: 1596–1604. https://doi.org/10.1016/j.bbagen.2013.09.017 PMID: 24060746
11. Almasalmeh A, Krenc D, Wu B, Beitz E. Structural determinants of the hydrogen peroxide permeability of aquaporins. FEBS J. 2014; 281: 647–656. https://doi.org/10.1111/febs.12653 PMID: 24286224

12. Wang H, Schoebel S, Schmitz F, Dong H, Hedfalk K. Characterization of aquaporin-driven hydrogen peroxide transport. Biochim Biophys Acta Biomembr BBA-BIOMEMBRANES. 2020; 1862: 183065. https://doi.org/10.1016/j.bbamem.2019.183065 PMID: 31521632

13. Miller EW, Dickinson BC, Chang CJ. Aquaporin-3 mediates hydrogen peroxide uptake to regulate downstream intracellular signaling. PNAS. 2010; 107: 15681–15686. https://doi.org/10.1073/pnas.1005776107 PMID: 20724658

14. Zinser ER. The microbial contribution to reactive oxygen species dynamics in marine ecosystems. Environ Microbiol Rep. 2018; 10: 412–427. https://doi.org/10.1111/1758-2229.12626 PMID: 29411545

15. Tjell AØ, Almdal K. Diffusion rate of hydrogen peroxide through water-swelled polyurethane membranes. Sensing and Bio-Sensing Research. 2018; 21: 35–39. https://doi.org/10.1016/j.sbsr.2018.10.001

16. Adesina AO, Sakugawa H. Photochemically generated nitric oxide in seawater: The peroxynitrite sink and its implications for daytime air quality. Sci Total Environ. 2021; 781: 146683. https://doi.org/10.1016/j.scitotenv.2021.146683 PMID: 33794463

17. Korshunov SS, Imlay JA. A potential role for periplasmic superoxide dismutase in blocking the penetration of external superoxide into the cytosol of Gram-negative bacteria. Mol Microbiol. 2002; 43: 95–106. https://doi.org/10.1046/j.1365-2958.2002.02719.x PMID: 11849539

18. Reinsberg PH, Koellisch A, Bawol PP, Baltruschat H. K_2 electrochemistry: Achieving highly reversible peroxide formation. Phys Chem Chem Phys. 2019; 21: 4286–4294. https://doi.org/10.1039/C8CP06362A PMID: 30724276

19. Tian Y, Yang G-P, Liu C-Y, Li P-F, Chen H-T, Bange HW. Photoproduction of nitric oxide in seawater. Ocean Sci. 2020; 16: 135–148. https://doi.org/10.5194/os-16-135-2020

20. Olasehinde EF, Takeda K, Sakugawa H. Photochemical Production and Consumption Mechanisms of Nitric Oxide in Seawater. Environ Sci Technol. 2010; 44: 8403–8408. https://doi.org/10.1021/es101426x PMID: 20954706

21. del Río LA, Puppo A, editors. Reactive oxygen species in plant signaling. Dordrecht; New York: Springer Verlag; 2009.

22. Zacharia IG, Deen WM. Diffusivity and Solubility of Nitric Oxide in Water and Saline. Ann Biomed Eng. 2005; 33: 214–222. https://doi.org/10.1007/s10439-005-8980-9 PMID: 15771275

23. Möller MN, Cuevasanta E, Orrico F, Lopez AC, Thomson L, Denicola A. Diffusion and Transport of Reactive Species Across Cell Membranes. In: Trostchansky A, Rubbo H, editors. Bioactive Lipids in Health and Disease. Cham: Springer International Publishing; 2019. pp. 3–19. https://doi.org/10.1007/978-3-030-11488-6_1 PMID: 31140168

24. Mopper K, Zhou X. Hydroxyl Radical Photoproduction in the Sea and Its Potential Impact on Marine Processes. Science. 1990; 250: 661–664. https://doi.org/10.1126/science.250.4981.661 PMID: 17810867

25. Sunday MO, Takeda K, Sakugawa H. Singlet Oxygen Photogeneration in Coastal Seawater: Prospect of Large-Scale Modeling in Seawater Surface and Its Environmental Significance. Environ Sci Technol. 2020; 54: 6125–6133. https://doi.org/10.1021/acs.est.0c00463 PMID: 32302118

26. Dill KA, Bromberg S. Molecular driving forces: Statistical thermodynamics in biology, chemistry, physics, and nanoscience. 2nd ed. London; New York: Garland Science; 2011.

27. Zielonka J, Sikora A, Joseph J, Kalyanaraman B. Peroxynitrite Is the Major Species Formed from Different Flux Ratios of Co-generated Nitric Oxide and Superoxide: DIRECT REACTION WITH BORONATE-BASED FLUORESCENT PROBE. J Biol Chem. 2010; 285: 14210–14216. https://doi.org/10.1074/jbc.M110.110080 PMID: 20194496

28. Marla SS, Lee J, Groves JT. Peroxynitrite rapidly permeates phospholipid membranes. PNAS. 1997; 94: 14243–14248. https://doi.org/10.1073/pnas.94.26.14243 PMID: 9405597

29. Hayyan M, Hashim MA, AlNashef IM. Superoxide Ion: Generation and Chemical Implications. Chem Rev. 2016; 116: 3029–3085. https://doi.org/10.1021/acs.chemrev.5b00407 PMID: 26875845

30. Fridovich I. Oxygen toxicity: A radical explanation. J Exp Biol. 1998; 201: 1203–1209. https://doi.org/10.1242/jeb.201.8.1203 PMID: 9510531

31. Winterbourn CC, Hampton MB. Thiol chemistry and specificity in redox signaling. Free Radic Biol Med. 2008; 45: 549–561. https://doi.org/10.1016/j.freeradbiomed.2008.05.004 PMID: 18544350

32. Roe KL, Barbeau KA. Uptake mechanisms for inorganic iron and ferric citrate in *Trichodesmium Erythraeum* IMS101. Metallomics. 2014; 6: 2042–2051. https://doi.org/10.1039/c4mt00026a PMID: 25222699

33. Rose A. The Influence of Extracellular Superoxide on Iron Redox Chemistry and Bioavailability to Aquatic Microorganisms. Front Microbiol. 2012; 3: 124. https://doi.org/10.3389/fmicb.2012.00124 PMID: 22514548

34. Kozuleva MA, Ivanov BN, Vetoshkina DV, Borisova-Mubarakshina MM. Minimizing an Electron Flow to Molecular Oxygen in Photosynthetic Electron Transfer Chain: An Evolutionary View. Front Plant Sci. 2020; 11: 211. https://doi.org/10.3389/fpls.2020.00211 PMID: 32231675

35. Blokhina O, Fagerstedt KV. Reactive oxygen species and nitric oxide in plant mitochondria: Origin and redundant regulatory systems. Physiologia Plantarum. 2010; 138: 447–462. https://doi.org/10.1111/j.1399-3054.2009.01340.x PMID: 20059731

36. Asada K, Kiso K, Yoshikawa K. Univalent Reduction of Molecular Oxygen by Spinach Chloroplasts on Illumination. J Biol Chem. 1974; 249: 2175–2181. https://doi.org/10.1016/S0021-9258(19)42815-9 PMID: 4362064

37. Kozuleva MA, Ivanov BN. Evaluation of the participation of ferredoxin in oxygen reduction in the photosynthetic electron transport chain of isolated pea thylakoids. Photosynth Res. 2010; 105: 51–61. https://doi.org/10.1007/s11120-010-9565-5 PMID: 20532996

38. Pospíšil P. Production of reactive oxygen species by photosystem II. Biochimica et Biophysica Acta (BBA)—Bioenergetics. 2009; 1787: 1151–1160. https://doi.org/10.1016/j.bbabio.2009.05.005 PMID: 19463778

39. Pospíšil P. The Role of Metals in Production and Scavenging of Reactive Oxygen Species in Photosystem II. Plant Cell Physiol. 2014; 55: 1224–1232. https://doi.org/10.1093/pcp/pcu053 PMID: 24771559

40. Solomon EI, Augustine AJ, Yoon J. O2 Reduction to H2O by the Multicopper Oxidases. Dalton Trans. 2008; 3921–3932. https://doi.org/10.1039/b800799c PMID: 18648693

41. Messner KR, Imlay JA. Mechanism of Superoxide and Hydrogen Peroxide Formation by Fumarate Reductase, Succinate Dehydrogenase, and Aspartate Oxidase. J Biol Chem. 2002; 277: 42563–42571. https://doi.org/10.1074/jbc.M204958200 PMID: 12200425

42. Mittler R. Oxidative stress, antioxidants and stress tolerance. Trends Plant Sci. 2002; 7: 405–410. https://doi.org/10.1016/s1360-1385(02)02312-9 PMID: 12234732

43. Zhang T, Hansel CM, Voelker BM, Lamborg CH. Extensive Dark Biological Production of Reactive Oxygen Species in Brackish and Freshwater Ponds. Environ Sci Technol. 2016; 50: 2983–2993. https://doi.org/10.1021/acs.est.5b03906 PMID: 26854358

44. Diaz JM, Hansel CM, Voelker BM, Mendes CM, Andeer PF, Zhang T. Widespread Production of Extracellular Superoxide by Heterotrophic Bacteria. Science. 2013; 340: 1223–1226. https://doi.org/10.1126/science.1237331 PMID: 23641059

45. Diaz JM, Plummer S, Tomas C, Alves-de-Souza C. Production of extracellular superoxide and hydrogen peroxide by five marine species of harmful bloom-forming algae. J Plankton Res. 2018; 40: 667–677. https://doi.org/10.1093/plankt/fby043 PMID: 30487659

46. Rose AL, Webb EA, Waite TD, Moffett JW. Measurement and Implications of Nonphotochemically Generated Superoxide in the Equatorial Pacific Ocean. Environ Sci Technol. 2008; 42: 2387–2393. https://doi.org/10.1021/es7024609 PMID: 18504970

47. Schneider RJ, Roe KL, Hansel CM, Voelker BM. Species-Level Variability in Extracellular Production Rates of Reactive Oxygen Species by Diatoms. Frontiers in Chemistry. 2016; 4. https://doi.org/10.3389/fchem.2016.00005 PMID: 27066475

48. Sutherland KM, Coe A, Gast RJ, Plummer S, Suffridge CP, Diaz JM, et al. Extracellular superoxide production by key microbes in the global ocean. Limnol Oceanogr. 2019; 64: 2679–2693. https://doi.org/10.1002/lno.11247

49. Kustka AB, Shaked Y, Milligan AJ, King DW, Morel FMM. Extracellular production of superoxide by marine diatoms: Contrasting effects on iron redox chemistry and bioavailability. Limnol Oceanogr. 2005; 50: 1172–1180. https://doi.org/10.4319/lo.2005.50.4.1172

50. Hansel CM, Buchwald C, Diaz JM, Ossolinski JE, Dyhrman ST, Mooy BASV, et al. Dynamics of extracellular superoxide production by *Trichodesmium Colonies from the Sargasso Sea*. Limnol Oceanogr. 2016; 61: 1188–1200. https://doi.org/10.1002/lno.10266

51. Marshall J-A, de Salas M, Oda T, Hallegraeff G. Superoxide production by marine microalgae. Mar Biol. 2005; 147: 533–540. https://doi.org/10.1007/s00227-005-1596-7

52. Sutherland KM, Grabb KC, Karolewski JS, Plummer S, Farfan GA, Wankel SD, et al. Spatial Heterogeneity in Particle-Associated, Light-Independent Superoxide Production Within Productive Coastal Waters. J Geophys Res Oceans. 2020; 125: e2020JC016747. https://doi.org/10.1029/2020JC016747 PMID: 33282615

53. Hansel CM, Diaz JM, Plummer S. Tight Regulation of Extracellular Superoxide Points to Its Vital Role in the Physiology of the Globally Relevant Roseobacter Clade. mBio. 2019; 10: e02668–18. https://doi.org/10.1128/mBio.02668-18 PMID: 30862752

54. Zafiriou OC. Chemistry of superoxide ion-radical (O2-) in seawater. I. (HOO) and uncatalyzed dismutation kinetics studied by pulse radiolysis. Mar Chem. 1990; 30: 31–43. https://doi.org/10.1016/0304-4203(90)90060-P

55. Sutherland KM, Wankel SD, Hansel CM. Dark biological superoxide production as a significant flux and sink of marine dissolved oxygen. PNAS. 2020; 117: 3433–3439. https://doi.org/10.1073/pnas.1912313117 PMID: 32015131

56. Wuttig K, Heller MI, Croot PL. Pathways of Superoxide (O2) Decay in the Eastern Tropical North Atlantic. Environ Sci Technol. 2013; 130826150409004. https://doi.org/10.1021/es401658t PMID: 23915117

57. Scanlan DJ, Ostrowski M, Mazard S, Dufresne A, Garczarek L, Hess WR, et al. Ecological Genomics of Marine Picocyanobacteria. Microbiol Mol Biol Rev. 2009; 73: 249–299. https://doi.org/10.1128/MMBR.00035-08 PMID: 19487728

58. Halliwell B, Gutteridge JMC. Free radicals in biology and medicine. 3rd ed. Oxford: New York: Clarendon Press; Oxford University Press; 1999.

59. Seaver LC, Imlay JA. Hydrogen peroxide fluxes and compartmentalization inside growing Escherichia Coli. J Bacteriol. 2001; 183: 7182–7189. https://doi.org/10.1128/JB.183.24.7182-7189.2001 PMID: 11717277

60. Fedurayev PV, Mironov KS, Gabrielyan DA, Bedbenov VS, Zorina AA, Shumskaya M, et al. Hydrogen Peroxide Participates in Perception and Transduction of Cold Stress Signal in Synechocystis. Plant Cell Physiol. 2018; 59: 1255–1264. https://doi.org/10.1093/pcp/pcy067 PMID: 29590456

61. Avery GB, Cooper WJ, Kieber RJ, Willey JD. Hydrogen peroxide at the Bermuda Atlantic Time Series Station: Temporal variability of seawater hydrogen peroxide. Mar Chem. 2005; 97: 236–244. https://doi.org/10.1016/j.marchem.2005.03.006

62. Kelly TJ, Daum PH, Schwartz SE. Measurements of peroxides in cloudwater and rain. Journal of Geophysical Research: Atmospheres. 1985; 90: 7861–7871. https://doi.org/10.1029/JD090iD05p07861

63. Willey JD, Kieber RJ, Lancaster RD. Coastal rainwater hydrogen peroxide: Concentration and deposition. J Atmos Chem. 1996; 25: 149–165. https://doi.org/10.1007/BF00053789

64. Morris JJ, Johnson ZI, Wilhelm SW, Zinser ER. Diel regulation of hydrogen peroxide defenses by open ocean microbial communities. J Plankton Res. 2016; 38: 1103–1114. https://doi.org/10.1093/plankt/fbw016

65. Yuan J, Shiller AM. The distribution of hydrogen peroxide in the southern and central Atlantic ocean. Deep Sea Research Part II: Topical Studies in Oceanography. 2001; 48: 2947–2970. https://doi.org/10.1016/S0967-0645(01)00026-1

66. Bond RJ, Hansel CM, Voelker BM. Heterotrophic Bacteria Exhibit a Wide Range of Rates of Extracellular Production and Decay of Hydrogen Peroxide. Front Mar Sci. 2020; 7: 72. https://doi.org/10.3389/fmars.2020.00072

67. Sengupta D, Mazumder S, Cole JV, Lowry S. Controlling Non-Catalytic Decomposition of High Concentration Hydrogen Peroxide: Fort Belvoir, VA: Defense Technical Information Center; 2004 Feb. https://doi.org/10.21236/ADA426795

68. Millero FJ, Sharma VK, Karn B. The rate of reduction of copper(II) with hydrogen peroxide in seawater. Mar Chem. 1991; 36: 71–83. https://doi.org/10.1016/S0304-4203(09)90055-X

69. Moffett JW, Zika RG. Reaction kinetics of hydrogen peroxide with copper and iron in seawater. Environ Sci Technol. 1987; 21: 804–810. https://doi.org/10.1021/es00162a012 PMID: 19995065

70. Vardi A, Formiggini F, Casotti R, De Martino A, Ribalet F, Miralto A, et al. A Stress Surveillance System Based on Calcium and Nitric Oxide in Marine Diatoms. PLoS Biol. 2006; 4: e60. https://doi.org/10.1371/journal.pbio.0040060 PMID: 16475869

71. Thomson PG. Ecophysiology of the brine dinoflagellate, Polarella Glacialis, and Antarctic fast ice brine communities. PhD thesis, University of Tasmania. 2000.

72. Vardi A, Bidle KD, Kwityn C, Hirsh DJ, Thompson SM, Callow JA, et al. A Diatom Gene Regulating Nitric-Oxide Signaling and Susceptibility to Diatom-Derived Aldehydes. Current Biology. 2008; 18: 895–899. https://doi.org/10.1016/j.cub.2008.05.037 PMID: 18538570

73. Vardi A. Cell signaling in marine diatoms. Commun Integr Biol. 2008; 1: 134–136. https://doi.org/10.4161/cib.1.2.6867 PMID: 19704870

74. Zafiriou OC, McFarland M, Bromund RH. Nitric Oxide in Seawater. Science. 1980; 207: 637–639. Available: https://www.jstor.org/stable/1683488 https://doi.org/10.1126/science.207.4431.637 PMID: 17749325

75. Fujiwara T, Fukumori Y. Cytochrome cb-type nitric oxide reductase with cytochrome c oxidase activity from Paracoccus denitrificans ATCC 35512. J Bacteriol. 1996; 178: 1866–1871. https://doi.org/10.1128/jb.178.7.1866-1871.1996 PMID: 8606159

76. Jahnová J, Luhová L, Petřivalský M. S-Nitrosoglutathione Reductase of Protein S-Nitrosation in Plant NO Signaling. Plants (Basel). 2019; 8: 48. https://doi.org/10.3390/plants8020048 PMID: 30795534

77. Collin F. Chemical Basis of Reactive Oxygen Species Reactivity and Involvement in Neurodegenerative Diseases. Int J Mol Sci. 2019;20. https://doi.org/10.3390/ijms20102407 PMID: 31096608

78. Marusawa H, Ichikawa K, Narita N, Murakami H, Ito K, Tezuka T. Hydroxyl radical as a strong electrophilic species. Bioorganic & Medicinal Chemistry. 2002; 10: 2283–2290. https://doi.org/10.1016/S0968-0896(02)00048-2 PMID: 11983525

79. Gutteridge JM. Reactivity of hydroxyl and hydroxyl-like radicals discriminated by release of thiobarbituric acid-reactive material from deoxy sugars, nucleosides and benzoate. Biochem J. 1984; 224: 761–767. https://doi.org/10.1042/bj2240761 PMID: 6098266

80. McGill MR, Jaeschke H. Chapter 4—Oxidant Stress, Antioxidant Defense, and Liver Injury. In: Kaplowitz N, DeLeve LD, editors. Drug-Induced Liver Disease (Third Edition). Boston: Academic Press; 2013. pp. 71–84. https://doi.org/10.1016/B978-0-12-387817-5.00004–2

81. Davies KJ, Goldberg AL. Proteins damaged by oxygen radicals are rapidly degraded in extracts of red blood cells. J Biol Chem. 1987; 262: 8227–8234. https://doi.org/10.1016/S0021-9258(18)47553-9 PMID: 3597373

82. Brezonik PL, Fulkerson-Brekken J. Nitrate-Induced Photolysis in Natural Waters: Controls on Concentrations of Hydroxyl Radical Photo-Intermediates by Natural Scavenging Agents. Environ Sci Technol. 1998; 32: 3004–3010. https://doi.org/10.1021/es9802908

83. Morris JJ, Lenski RE, Zinser ER. The Black Queen Hypothesis: Evolution of Dependencies through Adaptive Gene Loss. mBio. 2012; 3: e00036-12–e00036-12. https://doi.org/10.1128/mBio.00036-12 PMID: 22448042

84. Morris JJ, Johnson ZI, Szul MJ, Keller M, Zinser ER. Dependence of the Cyanobacterium Prochlorococcus on Hydrogen Peroxide Scavenging Microbes for Growth at the Ocean's Surface. Rodriguez-Valera F, editor. PLoS ONE. 2011; 6: e16805. https://doi.org/10.1371/journal.pone.0016805 PMID: 21304826

85. Zinser ER. Cross-protection from hydrogen peroxide by helper microbes: The impacts on the cyanobacterium Prochlorococcus and other beneficiaries in marine communities. Environ Microbiol Rep. 2018;0. https://doi.org/10.1111/1758-2229.12625 PMID: 29411546

86. Morris JJ, Kirkegaard R, Szul MJ, Johnson ZI, Zinser ER. Facilitation of Robust Growth of Prochlorococcus Colonies and Dilute Liquid Cultures by "Helper" Heterotrophic Bacteria. Appl Environ Microbiol. 2008; 74: 4530–4534. https://doi.org/10.1128/AEM.02479-07 PMID: 18502916

87. Coe A, Ghizzoni J, LeGault K, Biller S, Roggensack SE, Chisholm SW. Survival of Prochlorococcus in extended darkness. Limnol Oceanogr. 2016; 61: 1375–1388. https://doi.org/10.1002/lno.10302

88. Omar NM, Prášil O, McCain JSP, Campbell DA. Diffusional Interactions among Marine Phytoplankton and Bacterioplankton: Modelling H2O2 as a Case Study. Microorganisms. 2022; 10: 821. https://doi.org/10.3390/microorganisms10040821 PMID: 35456871

89. Mitchell JG, Seuront L, Doubell MJ, Losic D, Voelcker NH, Seymour J, et al. The Role of Diatom Nanostructures in Biasing Diffusion to Improve Uptake in a Patchy Nutrient Environment. PLoS One. 2013; 8: e59548. https://doi.org/10.1371/journal.pone.0059548 PMID: 23667421

90. DellaPenna D, Pogson BJ. VITAMIN SYNTHESIS IN PLANTS: Tocopherols and Carotenoids. Annual Review of Plant Biology. 2006; 57: 711–738. https://doi.org/10.1146/annurev.arplant.56.032604.144301 PMID: 16669779

91. Sharma P, Jha AB, Dubey RS, Pessarakli M. Reactive Oxygen Species, Oxidative Damage, and Antioxidative Defense Mechanism in Plants under Stressful Conditions. Journal of Botany. 2012; 2012: e217037. https://doi.org/10.1155/2012/217037

92. Database resources of the National Center for Biotechnology Information. Nucleic Acids Res. 2016; 44: D7–D19. https://doi.org/10.1093/nar/gkv1290 PMID: 26615191

93. Grigoriev IV, Nordberg H, Shabalov I, Aerts A, Cantor M, Goodstein D, et al. The Genome Portal of the Department of Energy Joint Genome Institute. Nucleic Acids Res. 2012; 40: D26–D32. https://doi.org/10.1093/nar/gkr947 PMID: 22110030

94. Nordberg H, Cantor M, Dusheyko S, Hua S, Poliakov A, Shabalov I, et al. The genome portal of the Department of Energy Joint Genome Institute: 2014 updates. Nucleic Acids Res. 2014; 42: D26–31. https://doi.org/10.1093/nar/gkt1069 PMID: 24225321

95. Youens-Clark K, Bomhoff M, Ponsero AJ, Wood-Charlson EM, Lynch J, Choi I, et al. iMicrobe: Tools and data-driven discovery platform for the microbiome sciences. GigaScience. 2019; 8. https://doi.org/10.1093/gigascience/giz083 PMID: 31289831

96. Leinonen R, Akhtar R, Birney E, Bower L, Cerdeno-Tárraga A, Cheng Y, et al. The European Nucleotide Archive. Nucleic Acids Res. 2011; 39: D28–D31. https://doi.org/10.1093/nar/gkq967 PMID: 20972220

97. Vandepoele K, Van Bel M, Richard G, Van Landeghem S, Verhelst B, Moreau H, et al. Pico-PLAZA, a genome database of microbial photosynthetic eukaryotes. Environ Microbiol. 2013; 15: 2147–2153. https://doi.org/10.1111/1462-2920.12174 PMID: 23826978

98. Matasci N, Hung L-H, Yan Z, Carpenter EJ, Wickett NJ, Mirarab S, et al. Data access for the 1,000 Plants (1KP) project. Gigascience. 2014; 3: 17. https://doi.org/10.1186/2047-217X-3-17 PMID: 25625010

99. Liew YJ, Aranda M, Voolstra CR. Reefgenomics.Org—a repository for marine genomics data. Database (Oxford). 2016; 2016. https://doi.org/10.1093/database/baw152 PMID: 28025343

100. Mölder F, Jablonski KP, Letcher B, Hall MB, Tomkins-Tinch CH, Sochat V, et al. Sustainable data analysis with Snakemake. F1000Research; 2021. https://doi.org/10.12688/f1000research.29032.2 PMID: 34035898

101. Huerta-Cepas J, Forslund K, Coelho LP, Szklarczyk D, Jensen LJ, von Mering C, et al. Fast Genome-Wide Functional Annotation through Orthology Assignment by eggNOG-Mapper. Mol Biol Evol. 2017; 34: 2115–2122. https://doi.org/10.1093/molbev/msx148 PMID: 28460117

102. Cantalapiedra CP, Hernández-Plaza A, Letunic I, Bork P, Huerta-Cepas J. eggNOG-mapper v2: Functional Annotation, Orthology Assignments, and Domain Prediction at the Metagenomic Scale. Bioinformatics; 2021 Jun. https://doi.org/10.1093/molbev/msab293 PMID: 34597405

103. Buchfink B, Xie C, Huson DH. Fast and sensitive protein alignment using DIAMOND. Nat Methods. 2015; 12: 59–60. https://doi.org/10.1038/nmeth.3176 PMID: 25402007

104. Huerta-Cepas J, Szklarczyk D, Heller D, Hernández-Plaza A, Forslund SK, Cook H, et al. eggNOG 5.0: A hierarchical, functionally and phylogenetically annotated orthology resource based on 5090 organisms and 2502 viruses. Nucleic Acids Research. 2019; 47: D309–D314. https://doi.org/10.1093/nar/gky1085 PMID: 30418610

105. Team RC. R: A Language and Environment for Statistical Computing. Vienna, Austria: R Foundation for Statistical Computing; 2019.

106. RStudio Team. RStudio: Integrated Development Environment for R. Boston, MA: RStudio, Inc.; 2015.

107. Wickham H. Tidyverse: Easily Install and Load the 'Tidyverse'. 2017.

108. Robinson D, Hayes A. Broom: Convert Statistical Analysis Objects into Tidy Tibbles. 2019.

109. Bache SM, Wickham H. Magrittr: A Forward-Pipe Operator for R. 2014.

110. Wickham H, François R, Henry L, Müller K. Dplyr: A Grammar of Data Manipulation. 2018.

111. Mangiafico S. Rcompanion: Functions to Support Extension Education Program Evaluation. 2020.

112. Warnes GR, Bolker B, Lumley T, Johnson R. Gmodels: Various R Programming Tools for Model Fitting. 2018.

113. Kleiber C, Zeileis A. AER: Applied Econometrics with R. 2020.

114. Warton DI, Duursma RA, Falster DS, Taskinen S. Smatr 3—an R package for estimation and inference about allometric lines. Methods in Ecology and Evolution. 2012; 3: 257–259.

115. Sauer S. Convert logit to probability. 2017.

116. Wickham H. Ggplot2: Elegant Graphics for Data Analysis. Springer-Verlag New York; 2016.

117. Wilke CO. Cowplot: Streamlined Plot Theme and Plot Annotations for 'Ggplot2'. 2019.

118. Hester J. Glue: Interpreted String Literals. 2018.

119. Zhu H. kableExtra: Construct Complex Table with 'kable' and Pipe Syntax. 2019.

120. Wei T, Simko V. R package "corrplot": Visualization of a Correlation Matrix. 2017.

121. Tang Y, Horikoshi M, Li W. Ggfortify: Unified Interface to Visualize Statistical Result of Popular R Packages. The R Journal. 2016; 8: 478–489.

122. Horikoshi M, Tang Y. Ggfortify: Data Visualization Tools for Statistical Analysis Results. 2018.

123. Pedersen TL, RStudio. Ggforce: Accelerating 'Ggplot2'. 2021.

124. Xie Y. Knitr AComprehensive Tool for Reproducible Research in R. Implementing Reproducible Research. Chapman and Hall/CRC; 2014.

125. Xie Y. Dynamic Documents with R and knitr. Second. Boca Raton, Florida: Chapman and Hall/CRC; 2015.

126. Xie Y. Knitr: A General-Purpose Package for Dynamic Report Generation in R. 2018.

127. Xie Y. Bookdown: Authoring books and technical documents with R markdown. 2019.

128. Aust F. Citr: 'RStudio' Add-in to Insert Markdown Citations. 2018.

129. Chang A, Jeske L, Ulbrich S, Hofmann J, Koblitz J, Schomburg I, et al. BRENDA, the ELIXIR core data resource in 2021: New developments and updates. Nucleic Acids Research. 2021; 49: D498–D508. https://doi.org/10.1093/nar/gkaa1025 PMID: 33211880

130. Lundgren CAK, Sjöstrand D, Biner O, Bennett M, Rudling A, Johansson A-L, et al. Scavenging of superoxide by a membrane-bound superoxide oxidase. Nat Chem Biol. 2018; 14: 788–793. https://doi.org/10.1038/s41589-018-0072-x PMID: 29915379

131. Matlashov ME, Belousov VV, Enikolopov G. How Much H2O2 Is Produced by Recombinant D-Amino Acid Oxidase in Mammalian Cells? Antioxid Redox Signal. 2014; 20: 1039–1044. https://doi.org/10.1089/ars.2013.5618 PMID: 24020354

132. Bou-Abdallah F, Yang H, Awomolo A, Cooper B, Woodhall MR, Andrews SC, et al. Functionality of the Three-Site Ferroxidase Center of Escherichia Coli Bacterial Ferritin (EcFtnA). Biochemistry. 2014; 53: 483–495. https://doi.org/10.1021/bi401517f PMID: 24380371

133. Fleury K. Reactive Oxygen Detoxification Genes in Phytoplankton. Bachelor of {{Science}}, {{Honors}} Thesis, Mount Allison University. 2019.

134. Omar N. Reactive Oxygen Production and Scavenging in Marine Phytoplankton. Bachelor of {{Science}}, {{Honors}} Thesis, Mount Allison University. 2020.

135. Shapiro SS, Wilk MB. An Analysis of Variance Test for Normality (Complete Samples). Biometrika. 1965; 52: 591. https://doi.org/10.2307/2333709

136. Anova.glm function—RDocumentation.

137. McFadden D. Quantitative Methods for Analyzing Travel Behaviour of Individuals: Some Recent Developments. Cowles Foundation Discussion Papers. 1977.

138. Kassambara A. Ggpubr: 'ggplot2' Based Publication Ready Plots. 2018.

139. Diaz JM, Plummer S, Hansel CM, Andeer PF, Saito MA, McIlvin MR. NADPH-dependent extracellular superoxide production is vital to photophysiology in the marine diatom *Thalassiosira Oceanica*. PNAS. 2019; 116: 16448–16453. https://doi.org/10.1073/pnas.1821233116 PMID: 31346083

140. Mella-Flores D, Six C, Ratin M, Partensky F, Boutte C, Le Corguillé G, et al. Prochlorococcus and Synechococcus have Evolved Different Adaptive Mechanisms to Cope with Light and UV Stress. Front Microbiol. 2012; 3: 285. https://doi.org/10.3389/fmicb.2012.00285 PMID: 23024637

141. Pospíšil P. Molecular mechanisms of production and scavenging of reactive oxygen species by photosystem II. Biochimica et Biophysica Acta (BBA)—Bioenergetics. 2012; 1817: 218–231. https://doi.org/10.1016/j.bbabio.2011.05.017 PMID: 21641332

142. Pospíšil P. Production of Reactive Oxygen Species by Photosystem II as a Response to Light and Temperature Stress. Frontiers in Plant Science. 2016;7. https://doi.org/10.3389/fpls.2016.01950 PMID: 28082998

143. Bergamini C, Gambetti S, Dondi A, Cervellati C. Oxygen, Reactive Oxygen Species and Tissue Damage. CPD. 2004; 10: 1611–1626. https://doi.org/10.2174/1381612043384664 PMID: 15134560

144. Miller A-F. Superoxide dismutases: Ancient enzymes and new insights. FEBS Lett. 2012; 586: 585–595. https://doi.org/10.1016/j.febslet.2011.10.048 PMID: 22079668

145. Groussman RD, Parker MS, Armbrust EV. Diversity and Evolutionary History of Iron Metabolism Genes in Diatoms. PLOS ONE. 2015; 10: e0129081. https://doi.org/10.1371/journal.pone.0129081 PMID: 26052941

146. Bernroitner M, Zamocky M, Furtmüller PG, Peschek GA, Obinger C. Occurrence, phylogeny, structure, and function of catalases and peroxidases in cyanobacteria. J Exp Bot. 2009; 60: 423–440. https://doi.org/10.1093/jxb/ern309 PMID: 19129167

147. Pandey P, Singh J, Achary VMM, Reddy MK. Redox homeostasis via gene families of ascorbate-glutathione pathway. Front Environ Sci. 2015;3. https://doi.org/10.3389/fenvs.2015.00025

148. Randhawa V, Thakkar M, Wei L. Applicability of Hydrogen Peroxide in Brown Tide Control Culture and Microcosm Studies. PLOS ONE. 2012; 7: e47844. https://doi.org/10.1371/journal.pone.0047844 PMID: 23082223

149. Picciano AL, Crane BR. A nitric oxide synthaselike protein from Synechococcus produces NO/NO3- from l-arginine and NAPDH in a tetrahydrobiopterin- and Ca2+-dependent manner. J Biol Chem. 2019; 294: 10708–10719. https://doi.org/10.1074/jbc.RA119.008399 PMID: 31113865

150. Zweier JL, Samouilov A, Kuppusamy P. Non-enzymatic nitric oxide synthesis in biological systems. Biochim Biophys Acta. 1999; 1411: 250–262. https://doi.org/10.1016/s0005-2728(99)00018-3 PMID: 10320661

151. Chen Y-C, Chen Y-H, Chiu H, Ko Y-H, Wang R-T, Wang W-P, et al. Cell-Penetrating Delivery of Nitric Oxide by Biocompatible Dinitrosyl Iron Complex and Its Dermato-Physiological Implications. Int J Mol Sci. 2021; 22: 10101. https://doi.org/10.3390/ijms221810101 PMID: 34576264

152. Lampe RH, Wang S, Cassar N, Marchetti A. Strategies among phytoplankton in response to alleviation of nutrient stress in a subtropical gyre. ISME J. 2019; 13: 2984–2997. https://doi.org/10.1038/s41396-019-0489-6 PMID: 31439897

153. Peifeng L, Min Z, Chunying L, Guipeng Y. Effects of Nitric Oxide On The Growth of The Marine Microalgae And The Parameters of Carbonate Chemistry. In Review; 2021 May. https://doi.org/10.21203/rs.3.rs-521371/v1

154. Thompson SEM, Taylor AR, Brownlee C, Callow ME, Callow JA. The Role of Nitric Oxide in Diatom Adhesion in Relation to Substratum Properties. J Phycol. 2008; 44: 967–976. https://doi.org/10.1111/j.1529-8817.2008.00531.x PMID: 27041615

155. Hunsucker KZ, Swain GW. In situ measurements of diatom adhesion to silicone-based ship hull coatings. J Appl Phycol. 2016; 28: 269–277. https://doi.org/10.1007/s10811-015-0584-7

156. Di Dato V, Musacchia F, Petrosino G, Patil S, Montresor M, Sanges R, et al. Transcriptome sequencing of three Pseudo-nitzschia species reveals comparable gene sets and the presence of Nitric Oxide Synthase genes in diatoms. Scientific Reports. 2015; 5: 1–14. https://doi.org/10.1038/srep12329 PMID: 26189990

157. Vihtakari M. ggOceanMaps: Plot Data on Oceanographic Maps using 'Ggplot2'. Zenodo; 2021. https://doi.org/10.5281/zenodo.4554715